APPLICATION OF ONE-DIMENSIONAL MIXING MODELS TO THE WINTER-TIME MEDITERRANEAN

by

DAVID ANDREA ANATI

B.S. The Hebrew University of Jerusalem

(1967)

SUBMITTED IN PARTIAL FULFILLMENT

OF THE REQUIREMENTS FOR THE

DEGREE OF MASTER OF SCIENCE

IN THE JOINT PROGRAM IN OCEANOGRAPHY

at the

MASSACHUSETTS INSTITUTE OF TECHNOLOGY

and the WOODS HOLE OCEANOGRAPHIC INSTITUTION

June, 1970

Signature of Author .....
Department of Earth and Planetary Sciences
June , 1970

Certified by .....
Thesis Supervisor

Accepted by .....
Chairman, Departmental Committee on
Graduate Students

CONTENTS

ABSTRACT

The buoyancies of three columns of water in the Northwest Mediterranean are compared at various stages of the mixed layer formation of February 1969.

The deepening of the mixed layer is shown to be of a non-penetrative character, and the adequacy of one-dimensional models is examined for this particular area and season.

INTRODUCTION

During the past few decades oceanographers have been speculating about the nature of the surface mixed layer. This is a layer, characterized by homogeneous salinity and potential temperature, that extends from the surface to a depth varying from practically zero (in the absence of such a layer) to a few hundreds of meters, and in extreme cases to a depth of one or two kilometers.

Three main processes may contribute to its formation and deepening:

1) Excess of evaporation over precipitation, i.e., increase in salinity and consequently increase in density.
2) Cooling of the top layer due to heat loss to the atmosphere (sensible and latent), and radiation effect. Again increase in density.
3) Mechanical stirring of the top layer, mainly by wind.

Some theories were advanced by various authors, and will be reviewed briefly in the next chapter, but oceanic measurements needed to verify or dismiss such theories were so scarce that no definite conclusion could be drawn by comparing predictions with evidence.

During the winter of 1969 a multiple ship survey, including six research vessels from four countries, was carried out in the northwest Mediterranean in the area of strong vertical mixing. This survey, the so-called MEDOC '69, gives perhaps the first opportunity to

oceanographers to look into the details of the processes involved, and to check with a somewhat higher degree of certainty all the theories that had previously been mostly in the speculative stage.

The present work considers mainly three of the many questions so crucial to the understanding of the formation and deepening of this mixed layer:

1) To what extent is the process of the penetrative kind rather than the non-penetrative?
2) What is the relative importance of each of the three mechanisms listed above, namely, evaporation, heat flux, and mechanical energy flux?
3) To what extent can any one-dimensional model be sufficient to explain the phenomenon in question?

This work does not by any means intend to conclusively solve these questions as related to the general problem of the formation and deepening of the mixed layer. Indeed, we must bear in mind that different processes might be important in different geographical areas or during different seasons, and therefore the results of the present investigation can apply with some reliability only to this particular location and this particular time of the year, that is, until we find further evidence of a similar situation somewhere else.

REVIEW OF PREVIOUS WORKS

A description of the surface mixed layer is given by Rossby and Montgomery (1935) in a discussion of the layers of frictional influence. It has been shown qualitatively (Francis and Stommel, 1953) and later quantitatively (Tabata, Boston and Boyce, 1965) that the depth of this mixed layer is highly correlated to the wind speed. This later thorough study of this problem, based on observations taken at station P in the Pacific Ocean, does not deal however with the question of how the wind affects this process: whether by directly stirring the upper layers of the ocean, or indirectly by enhancing evaporation rates and sensible heat flux from the ocean to the atmosphere.

Kraus and Rooth (1961) on the other hand consider the problem mainly from the heat-flux point of view, and advance a model that considers a steady state and includes a brief discussion of some cases of transient development. This paper emphasizes the difficulty in determining to what extent the bottom of the mixed layer overshoots the limit of neutral stability by penetration into the otherwise quiescent waters below.

This penetrative behaviour was reported to occur in the atmospheric equivalent of this problem by Ball (1960). It was assumed to occur in the ocean by Kraus and Turner (1965) in their model of the seasonal thermocline in which they neglect entirely the mechanical stirring but take the heat flux as responsible for generation

of kinetic energy, and its further transformation into potential energy by penetrative convection.

This treatment is an improvement over preceding models in that it includes the time-dependence previously omitted.

In dealing with this problem we cannot ignore the importance of laboratory experiments performed by these authors, as well as by Rouse and Dodu (1955), Cromwell (1960) and finally by Kato and Phillips (1969). This last experiment, in which an initially stable stratification was stirred from the top surface, is particularly relevant to the present work since its numerical results were used in estimating the mechanical energy flux W as explained in Appendix A.

The particular area from which our oceanic measurements were taken, the Northwest Mediterranean, has attracted the attention of physical oceanographers for its narrow region of very deep penetration of the mixed layer in winter. Saint-Guily (1961) showed that a cyclonic gyre could account for the weak stability encountered in this area just before the onset of the mistral, and this idea has been mentioned also in the Medoc group report (1970) and by Stommel (1970). Both papers, as well as Anati and Stommel (1970), describe in detail the various phases that the deepening of the mixed layer goes through and include many salinity sections to which we shall refer later.

It is important to remember that all models reviewed here were basically one-dimensional models. Thus, for example, Francis and Stommel (1953) purposely discard data from areas where the

horizontal gradients are suspected to be non-negligible. Kraus and Rooth (1961) admit that "A full answer to the problem requires a three-dimensional" picture but, they say, the aim of their discussion is "more modest". Similarly, Kraus and Turner (1965) have to assume that "all the heat and mechanical energy which affect the water column can be put in near the surface and propagated downwards, without being influenced significantly by horizontal velocities, advection, or rotation". We shall return to this point in our conclusions.

THE CHOICE OF THE STATIONS

For the Northwest Mediterranean it has become customary to use the salinity as the main indicator of the mixed layer, and indeed salinity sections show rather clearly the depth and width of this homogeneous body of water. For the dynamic problem on hand, however, the buoyancy seems to be a more adequate indicator, since we deal with the stability problem. Thus, for the rest of the present work, the standard indicator will be the negative buoyancy, defined as*

$$b \equiv g \frac{\rho - \tilde{\tilde{\rho}}}{\tilde{\tilde{\rho}}}$$

Here ρ is the observed density and $\tilde{\tilde{\rho}} = \tilde{\tilde{\rho}}(z)$ is a potential density computed from the Tumlirz equation of state using an average salinity and potential temperature. b is therefore expected to be entirely homogeneous in a thoroughly mixed region.

For the purpose of comparison, the reference density $\tilde{\rho}(z)$ must be one common to all stations involved. Since this $\tilde{\rho}(z)$ was computed for each station using the station's own pressures, this might give rise to dangerous discrepancies between these reference densities. To ensure that this does not actually happen, the reference densities of all the stations involved were plotted on a common diagram. Figure 1 shows the departure from the mean reference density. Clearly, we may feel confident that these discrepancies are far smaller than the needed accuracy.

---

* Negative buoyancy will occasionally be referred to as buoyancy.

Being reassured now that all stations have a common reference density we may proceed to the choice of the stations. Among all those available, a number of stations have been selected with the following criteria: first of all, we must cover a period that includes the onset of the mistral (with measurements taken just before the onset) and continues for the first period of deepening of the mixed layer. Second, we want to choose the stations in such a way that they will be arranged as time sequences of the same column of water, or at least of columns located as close as possible to the same place.

The chosen stations are shown in figure 2. The horizontal axis is time, covering the first half of the month of February 1969. In the lower part of the diagram, the evaporation-rate E, heat-flux H, and mechanical energy input W, as estimated by the methods described in Appendix A, are plotted against time. The calm period during the first days is clearly detectable, as is the stormy period that follows the onset of the mistral on the night of the third of February. At the top of the diagram three sections of three stations each are shown, together with one additional station between sections 1 and 2. The numbers refer to the original station numbers. All stations are Atlantis II stations with the exception of 6753 and 6759 which are Discovery stations.

At the center of the diagram the locations of these stations are shown with respect to the center of the mixed layer as estimated by the salinity cross sections described by Anati and Stommel (1970). Scales for the distance from this center are shown at the left of

the diagram.

We immediately notice that section 3 is narrower than we would like, and in fact, we shall regret later the absence of a station south of station 6759. For the time being it suffices to remember that station 6759 is too close to the center of the mixed layer and therefore we would expect it to show a somewhat more advanced state of mixing than the development of station 6753.

Unfortunately our data did not include any stations north and south of station 1310 which were reasonably closely-spaced in time.

The above-mentioned choice gives us three sequences:

Northern sequence:	1302	-		1316	-	1322
Central sequence:	1303	-	1310	- 1317	-	1320
Southern sequence:	1305	-		6753	-	6759

The buoyancies for each of these sequences are shown in figures 3a, 3b, and 3c.

In order to give a clearer idea of the two-dimensional picture, the three schematic sections are shown in figures 4a, 4b, and 4c. With perhaps the exception, as expected, of station 6759, the three sections are easily acceptable qualitatively as a time-sequence of the same section under the effect of a buoyancy flux through the surface.

With these observed profiles on hand, we may now proceed to compare various predictions with oceanic evidence.

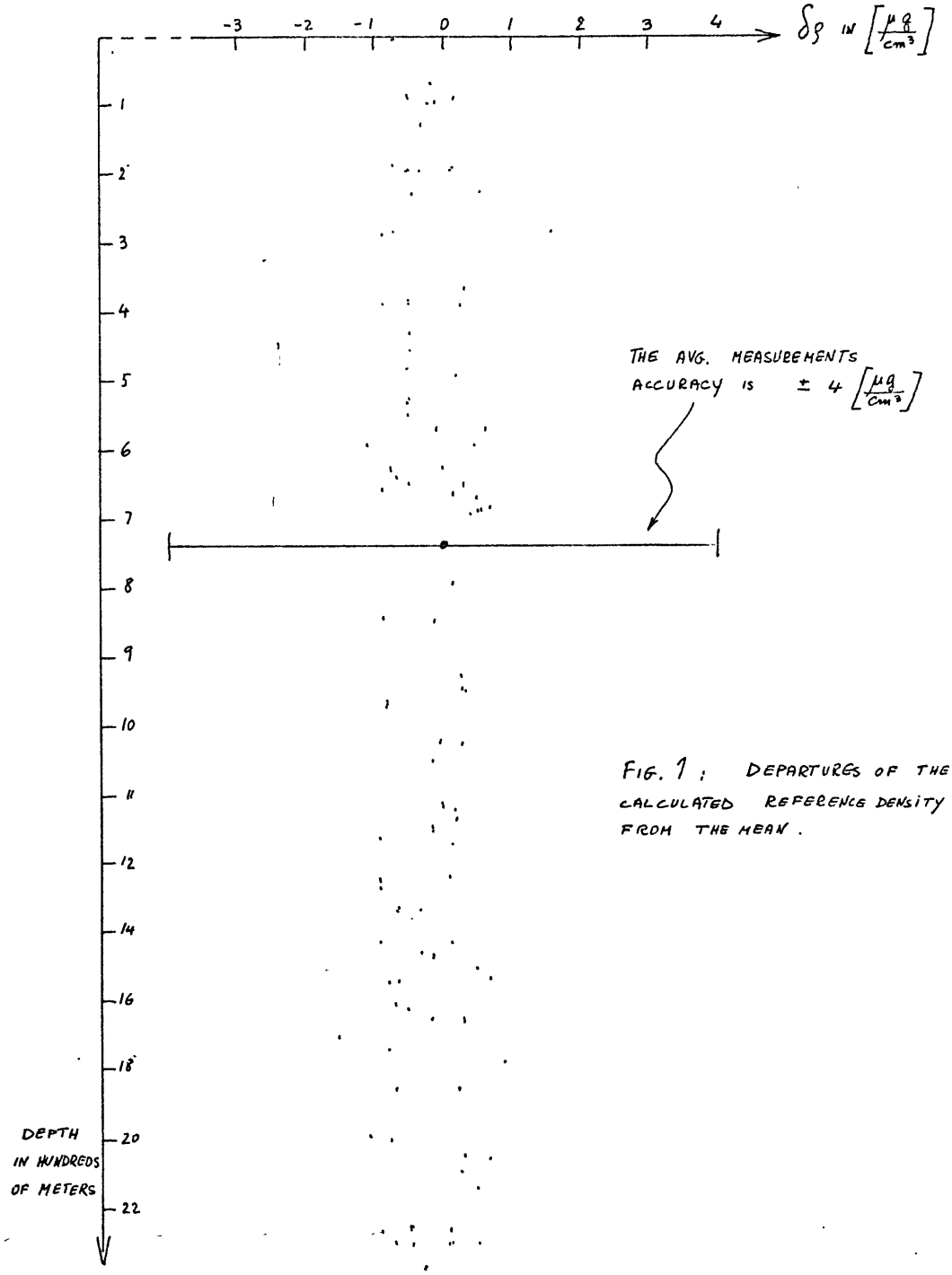

FIG. 1 : DEPARTURES OF THE CALCULATED REFERENCE DENSITY FROM THE MEAN .

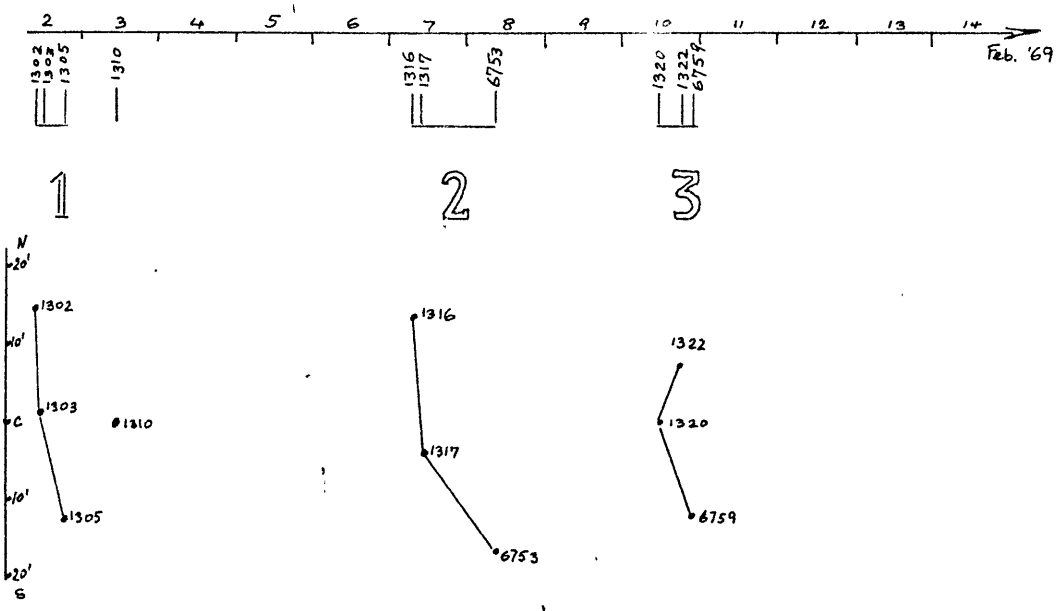
2 3 4 5 6 7 8 9 10 11 12 13 14
Feb. '69
1302
1303
1305
1310
1316
1317
6753
1320
1322
6759
1
2
3
N
20'
10'
C
10'
20'
S
1302
1303
1310
1305
1316
1317
6753
1322
1320
6759

FIG. 2 LEGEND:

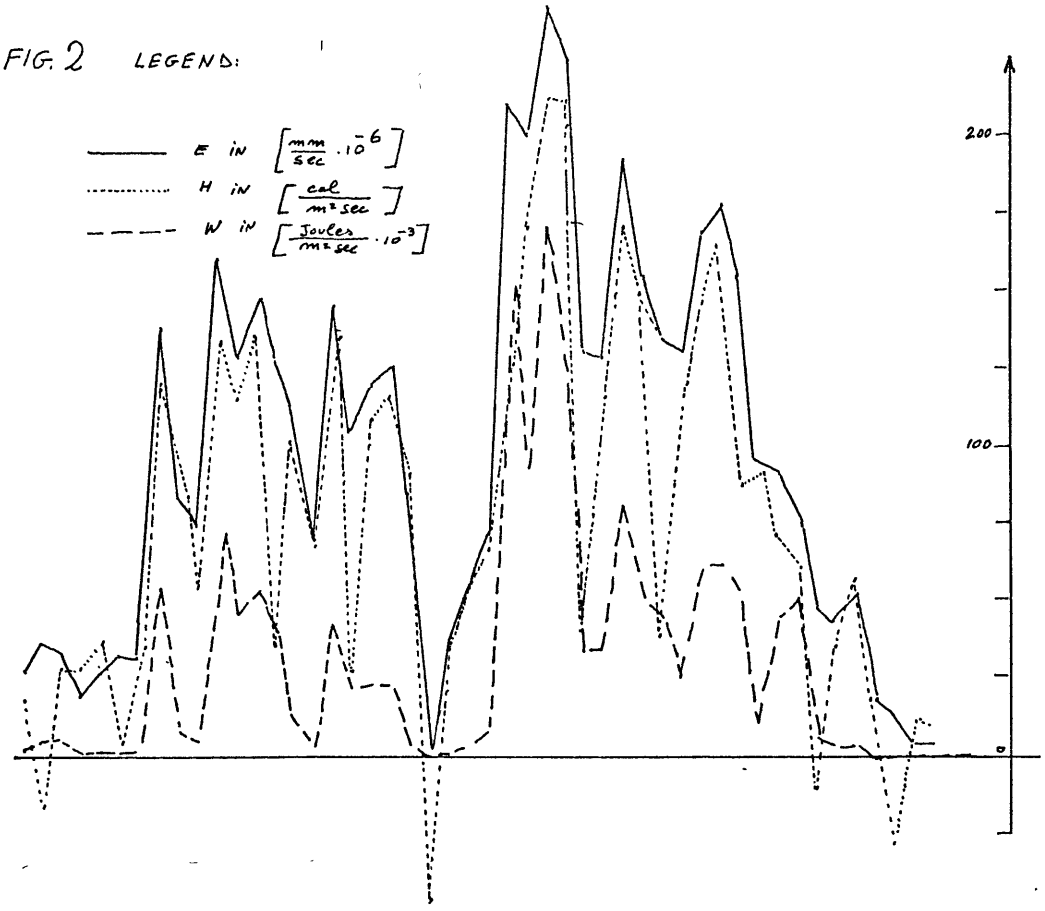
E in $\left[\frac{mm}{sec} \cdot 10^{-6}\right]$
H in $\left[\frac{cal}{m^2 sec}\right]$
W in $\left[\frac{Joules}{m^2 sec} \cdot 10^{-3}\right]$
200
100
0

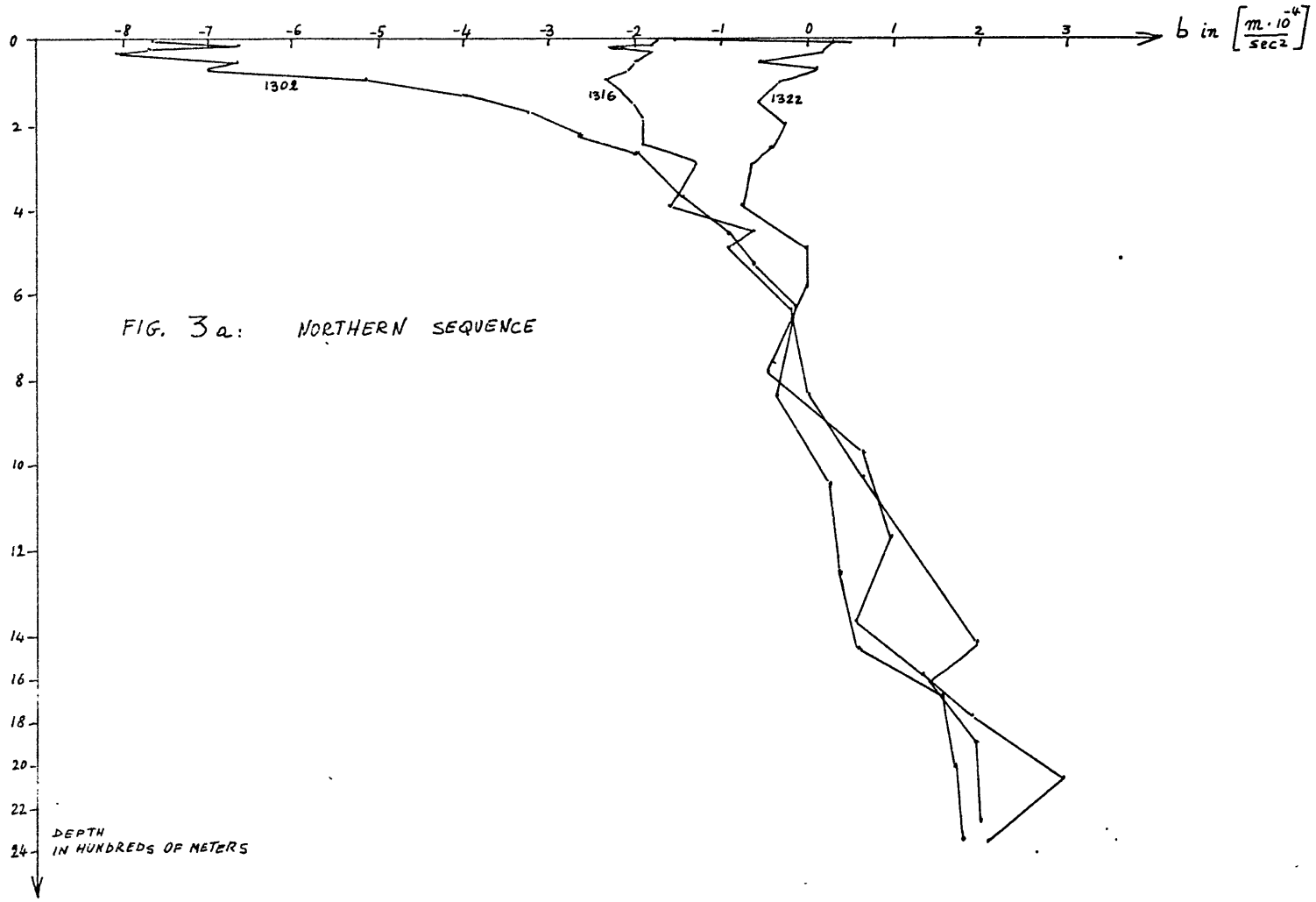

FIG. 3a: NORTHERN SEQUENCE

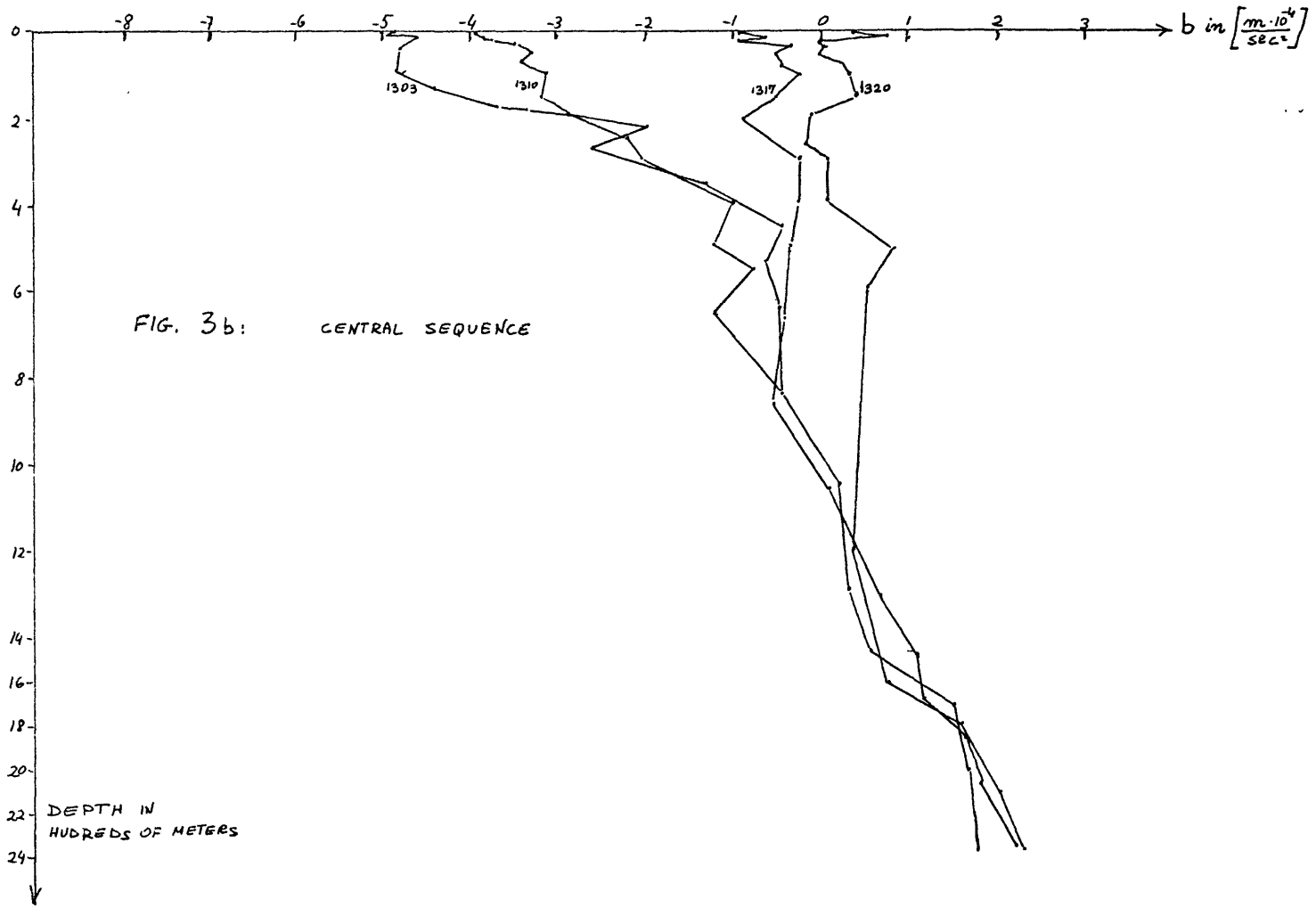

FIG. 3b: CENTRAL SEQUENCE

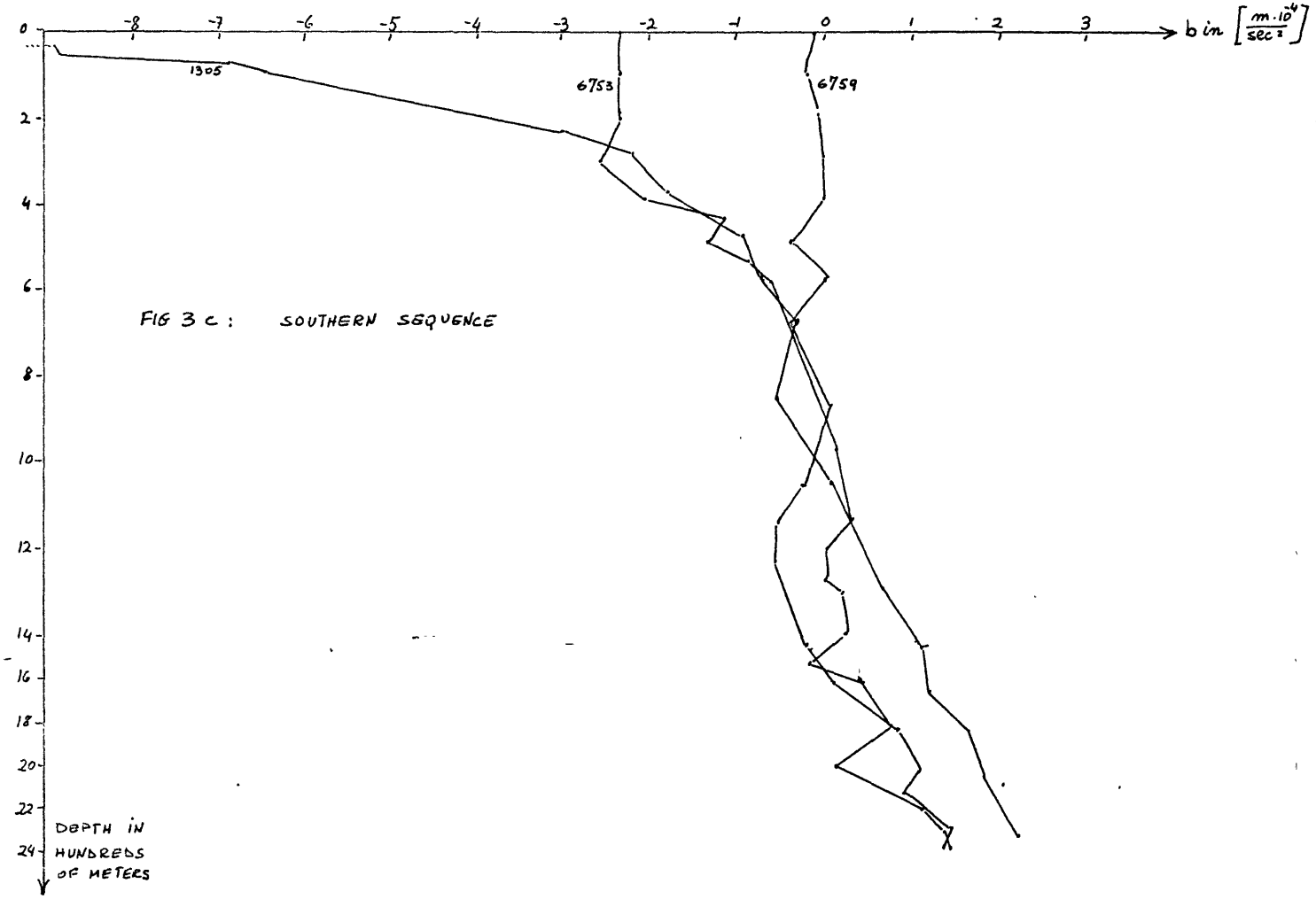

FIG 3 c : SOUTHERN SEQUENCE

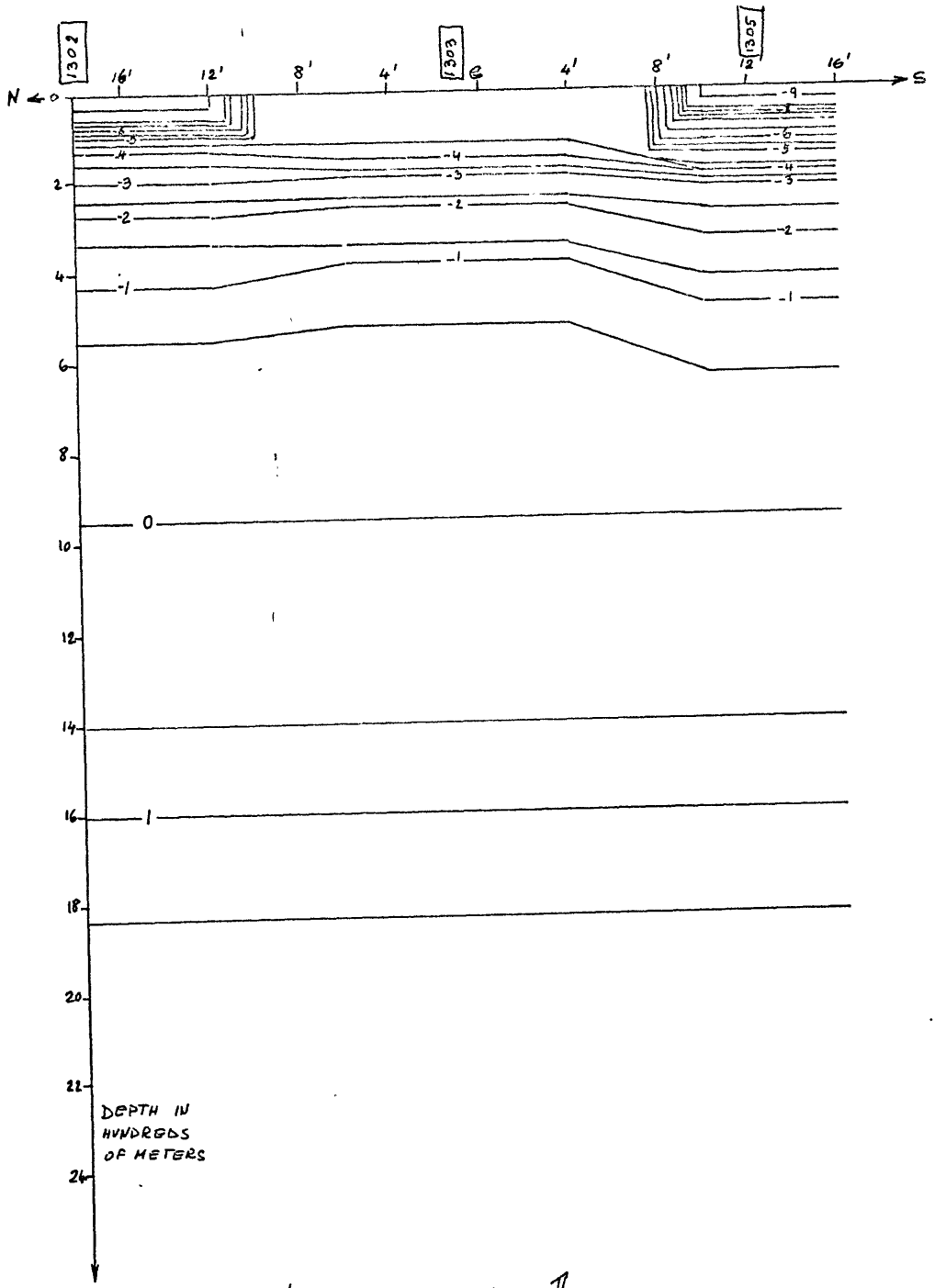

FIG. 4a : SECTION 1

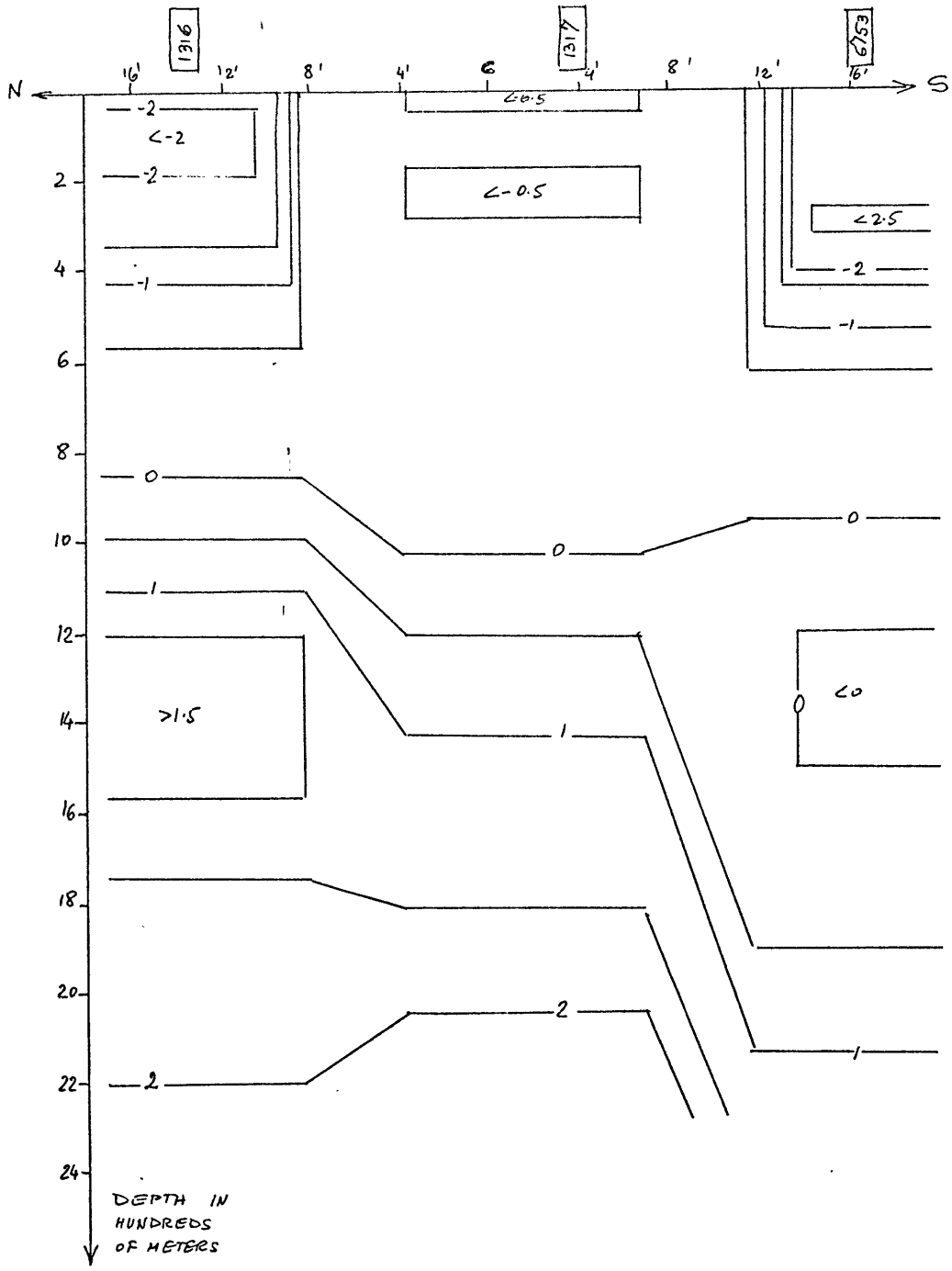

FIG. 4b: SECTION 2

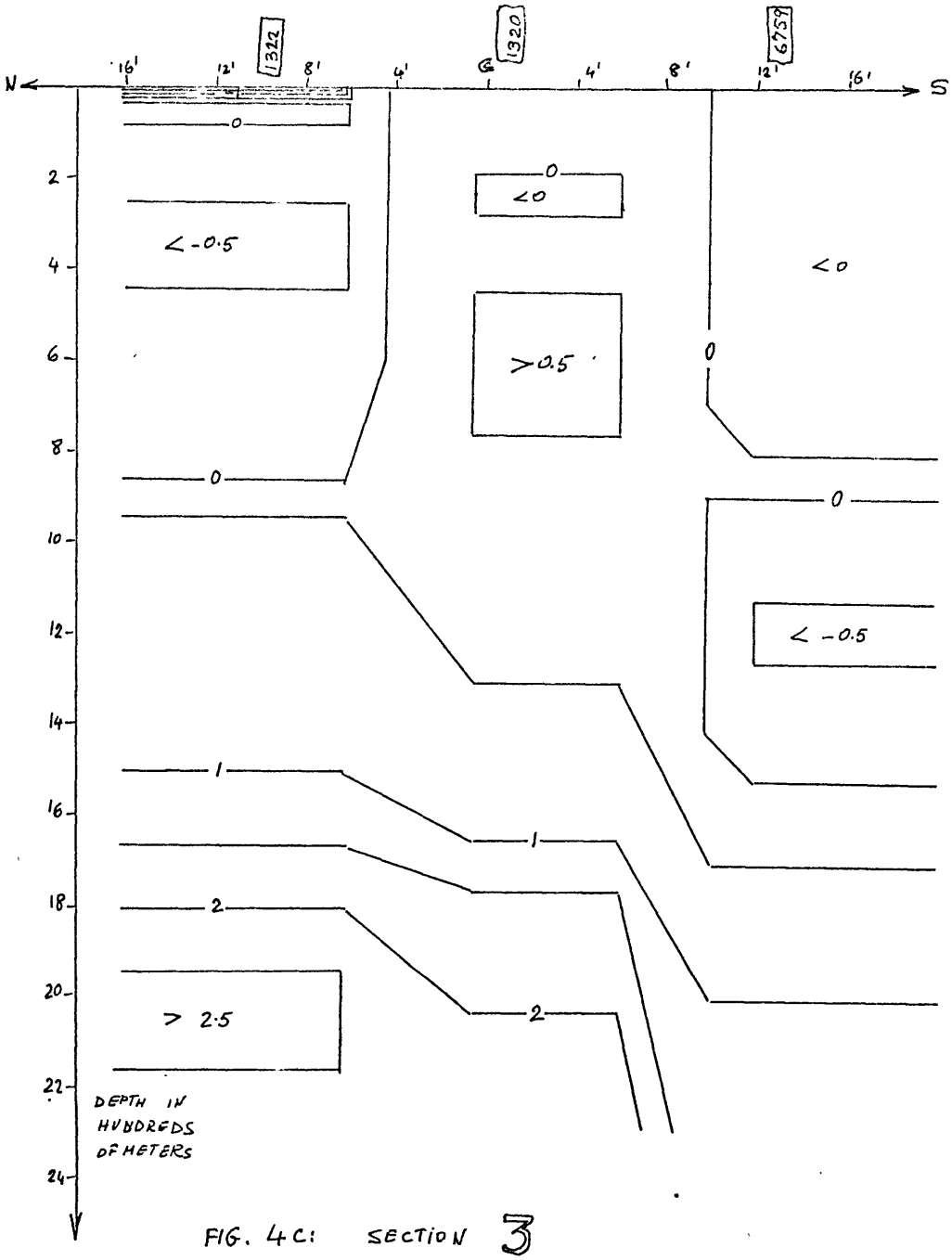

FIG. 4C: SECTION 3

THE PENETRATIVE MODEL

By "penetrative" deepening of the mixed layer, we mean a process in which entrainment of water from below into the mixed layer occurs. Starting with a linearly stratified column, a typical profile would look like figure 5a for a penetrative deepening, and like figure 5b for a non-penetrative deepening.

We now want to check how well a penetrative model can predict the observed development. In order to test our data with this question in mind, I have used a formulation of Ball's model (1960) developed for this purpose by N. Phillips. To briefly introduce the model (explained in detail in appendix B), consider the following simplification: suppose we have a linear stratification as our initial conditions:

$$\rho(z) = \rho_0 + \Gamma z \quad .$$

A mixed layer is formed, and say that after sometime it reaches the depth D. Denote:

$$\Delta\rho = \rho(D) - \rho_0 = \Gamma D \quad .$$

At one extreme we have the case where no cooling or evaporation occurs at all, and the mixed layer so formed is entirely the consequence of mechanical stirring. By conservation of mass, we have in this case a jump in density at the bottom of the mixed layer of

magnitude

$$\delta \rho = \frac{\Gamma D}{2}$$

(see figure 5c) and the potential energy of the column is increased by

$$\Delta V = g \frac{\Gamma D^3}{12} > 0 .$$

At the other extreme we have the case where no jump in density occurs at all at the bottom of the mixed layer. This is the equivalent of evenly cooling the mixed layer in an ideally non-turbulent way so that it deepens, as time advances, exactly at the limit of instability (see figure 5b). In this case the potential energy is decreased by:

$$\Delta V = -g \frac{\Gamma D^3}{6} < 0 .$$

As an intermediate case we can take a process in which the potential energy is conserved:

$$\Delta V \equiv 0 ,$$

which gives a jump in density of $\delta \rho = \frac{\Gamma D}{6}$ (see figure 5d).

Phillips followed Ball in assuming that in the absence of any mechanical stirring, i.e. in the case $W = 0$, we have $\Delta V \equiv 0$. Any increase in potential energy is therefore entirely due to mechanical stirring.

Let $\bar{b}(t)$ and $h(t)$ define the (negative) buoyancy and depth of the mixed layer, and let $b_e(z)$ denote the original buoyancy distribution with depth. The assumed conversion of all mechanical stirring (W) into potential energy gives the relation

$$h\, b_e(h) \frac{dh}{dt} - \frac{1}{2} \frac{d}{dt}\left(\bar{b} h^2\right) = \frac{W}{\rho_0}$$

The effect of evaporation (E) and upward heat flux (H) at the surface is to increase the mixed layer density. H includes the latent heat for evaporation. We may write (approximately)

$$\rho = \rho_0 \left(1 - \alpha T + \beta S \right)$$

for the dependence of ρ on temperature T and salinity S, with suitable constant values for α and β. The effect of E and H on the buoyancy of the column is then given by

$$\frac{d}{dt}\left(h \bar{b}\right) - b_e(h) \frac{dh}{dt} = g \left[\beta S^* E + \frac{\alpha}{c} H \right]$$

where S^* is a suitable mean surface salinity and C is the specific heat (4.18×10 ergs $gm^{-1}deg^{-1}$). $b_e(h)$ can be taken as a piece-wise linear function of h between successive points on a sounding. These two equations can then be readily solved numerically for $\bar{b}(t)$ and $h(t)$ if the forcing functions W, E, and H are known. Details are reproduced in Appendix B.

The fluxes E, H, and W, estimated as explained in Appendix A, were applied with this model to the various stations for the same

periods of time as observed, and the results are shown in figures 6a, 6b, and 6c. The number in parentheses denotes the time lapsed between the two compared stations.

For the north and south sequences, the results seem to show that the predicted mixed layer is too deep and its buoyancy is too great (with the exception of station 6759 which, as already pointed out, we expected to be somewhat too advanced in the penetration). For the center sequence the prediction seems to be better.

At this stage we are tempted to ask the following question: is it possible that the model is correct but that the fluxes E, H, and W are wrong? It will be shown later, following a different test, that our flux estimates are not as bad as that, but at present we have reasons to doubt the accuracy of these flux estimates: for one thing, we see in Appendix A that different authorities differ in their opinion by as much as a factor of 1.4 on the coefficient C_{DR}, and the mere fact that different prominent scientists disagree on the basic fact of whether or not this C_{DR} is a function of the wind velocity shows us clearly that, whatever approach we adopt, our estimates are far from certain.

We have a way to circumvent this difficulty though. Let's take the actual observed buoyancy, and compute the depth which would fit with this buoyancy, and the time required to reach this buoyancy according to our model. If the depth and buoyancy will be consistent with each other, then the appropriate changes in the times will compensate for errors in the flux estimates, and we may have some more

confidence in the model.*

The results are shown in figures 7a, 7b, and 7c. The two numbers in parentheses denote again the time in days: the one near the station numbers is the observed time; the one below, the computed one. The predictions show consistently that the mixed layer is too deep and the computed times are too short.

A similar additional test was done, taking now the observed depth as our standard, and the results are displayed in figures 8a, 8b, and 8c. Even a quick glance shows us that we cannot be satisfied with this model - all stations, with no exception, show a predicted buoyancy much less than observed.

As a final criterion to test this penetrative model, let's plot together on the same diagram the three different predictions: the one taking the same time as observed, the one taking the same buoyancy as observed, and the one taking the same depth as observed, and see how scattered the various predictions are.

The results are shown in figures 9a, 9b, and 9c. The great spread is obvious and reluctantly we have to reject the penetrative model, at least for this particular area and season.

---

* By "the actual observed buoyancy" we mean the averaged observed buoyancy from the surface to the approximate depth where the two compared curves intersect.

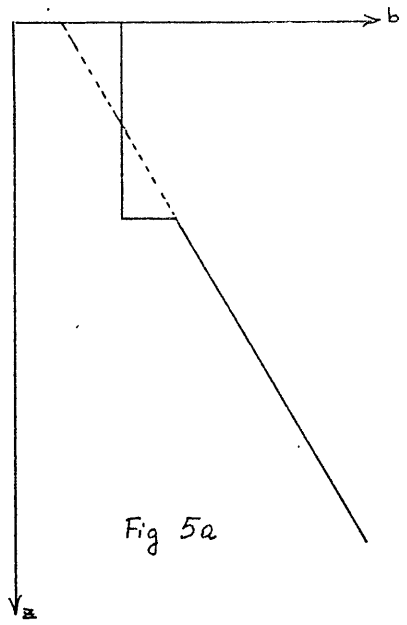

Fig 5a

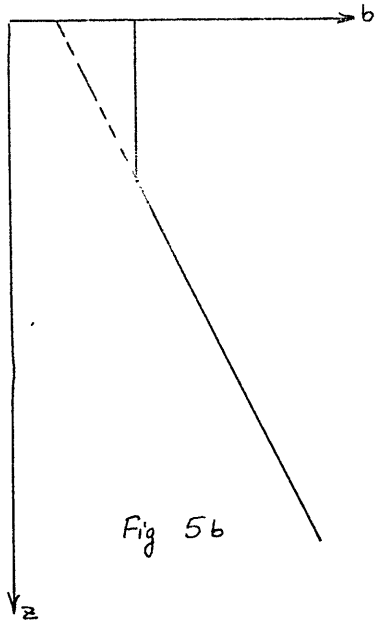

Fig 5b

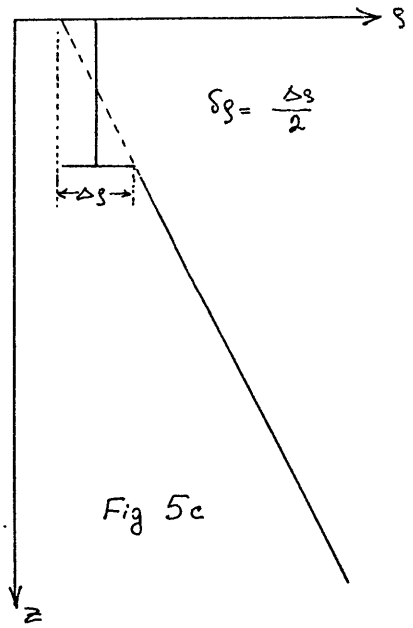

Fig 5c

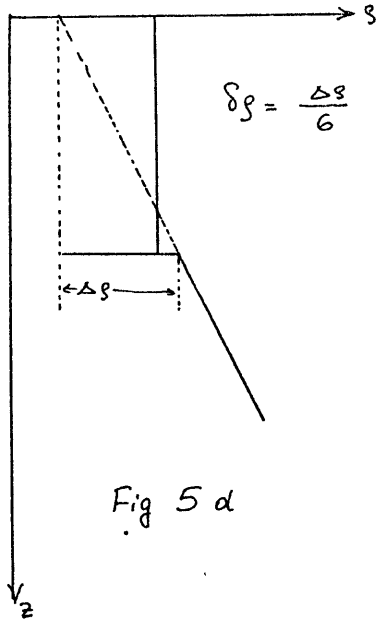

Fig 5d

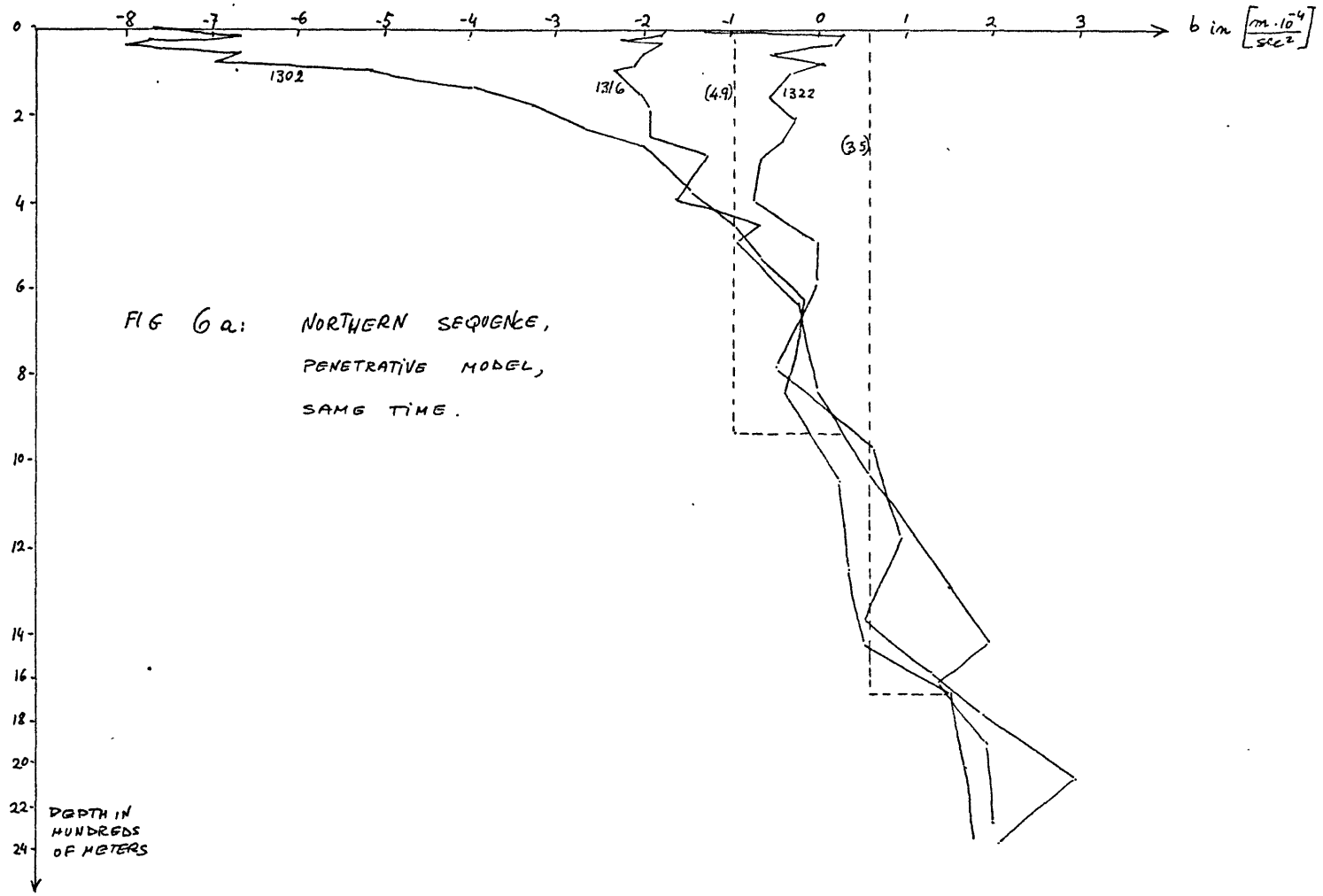

FIG 6a: NORTHERN SEQUENCE, PENETRATIVE MODEL, SAME TIME.

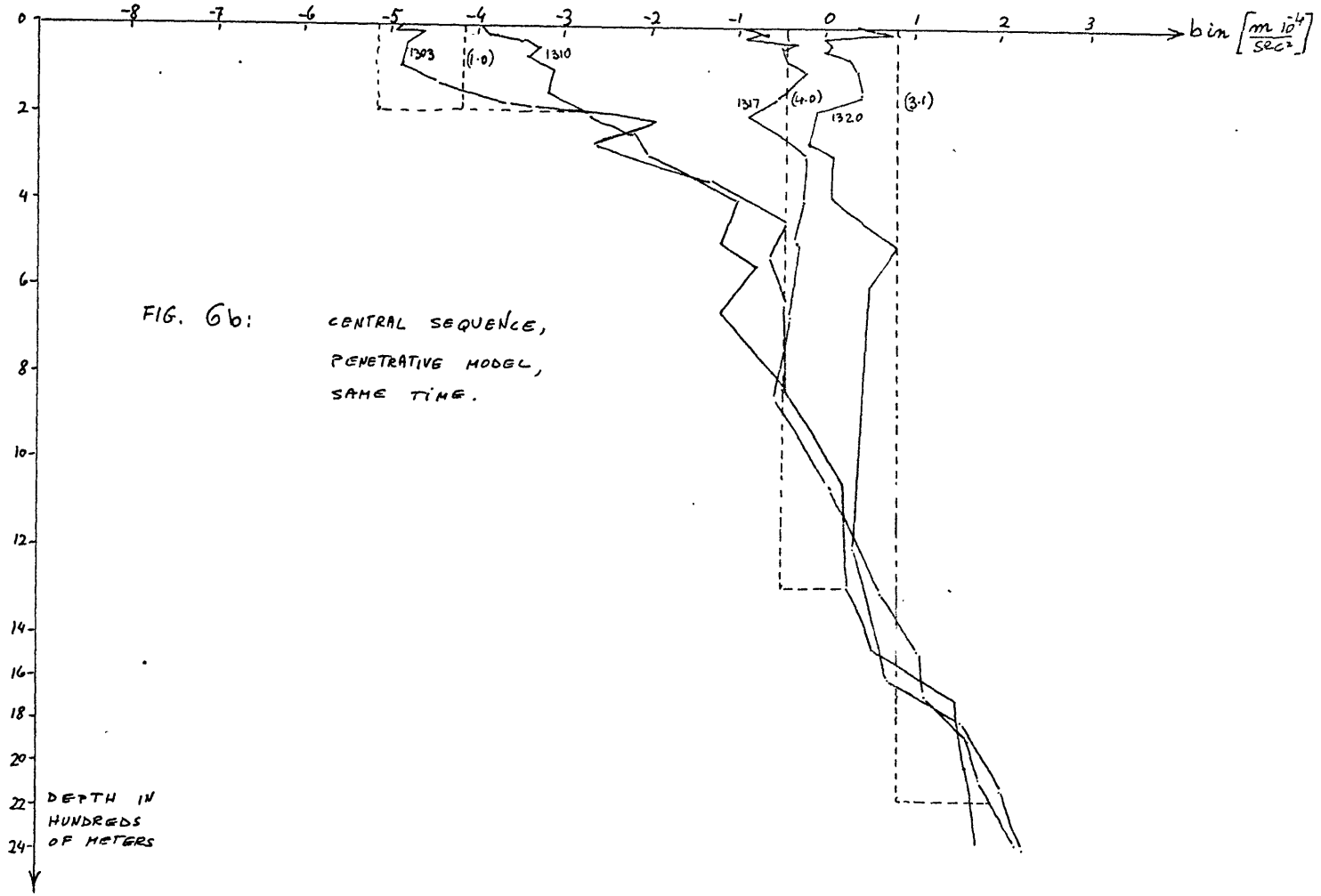

FIG. 6b: CENTRAL SEQUENCE, PENETRATIVE MODEL, SAME TIME.

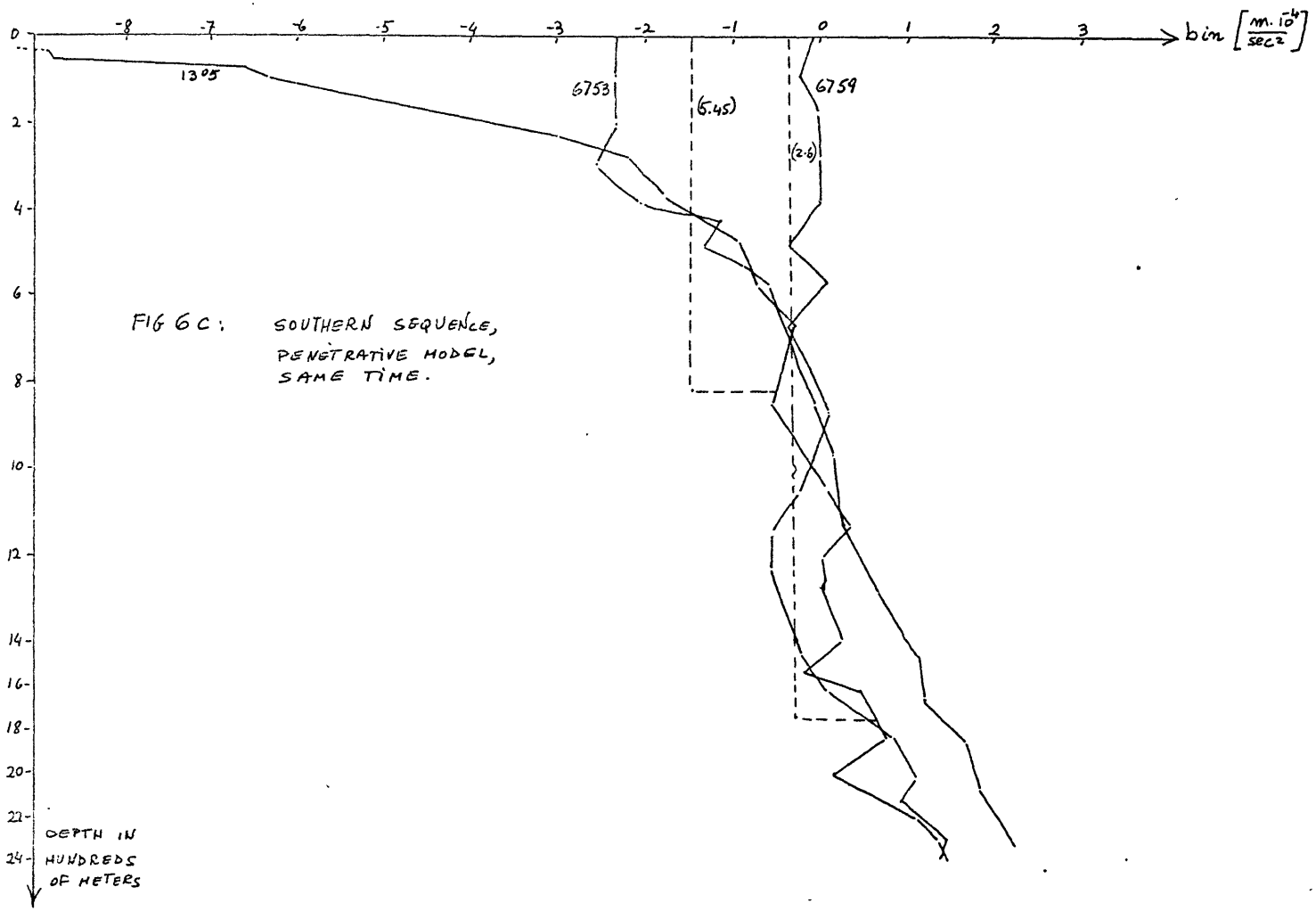

FIG 6C: SOUTHERN SEQUENCE, PENETRATIVE MODEL, SAME TIME.

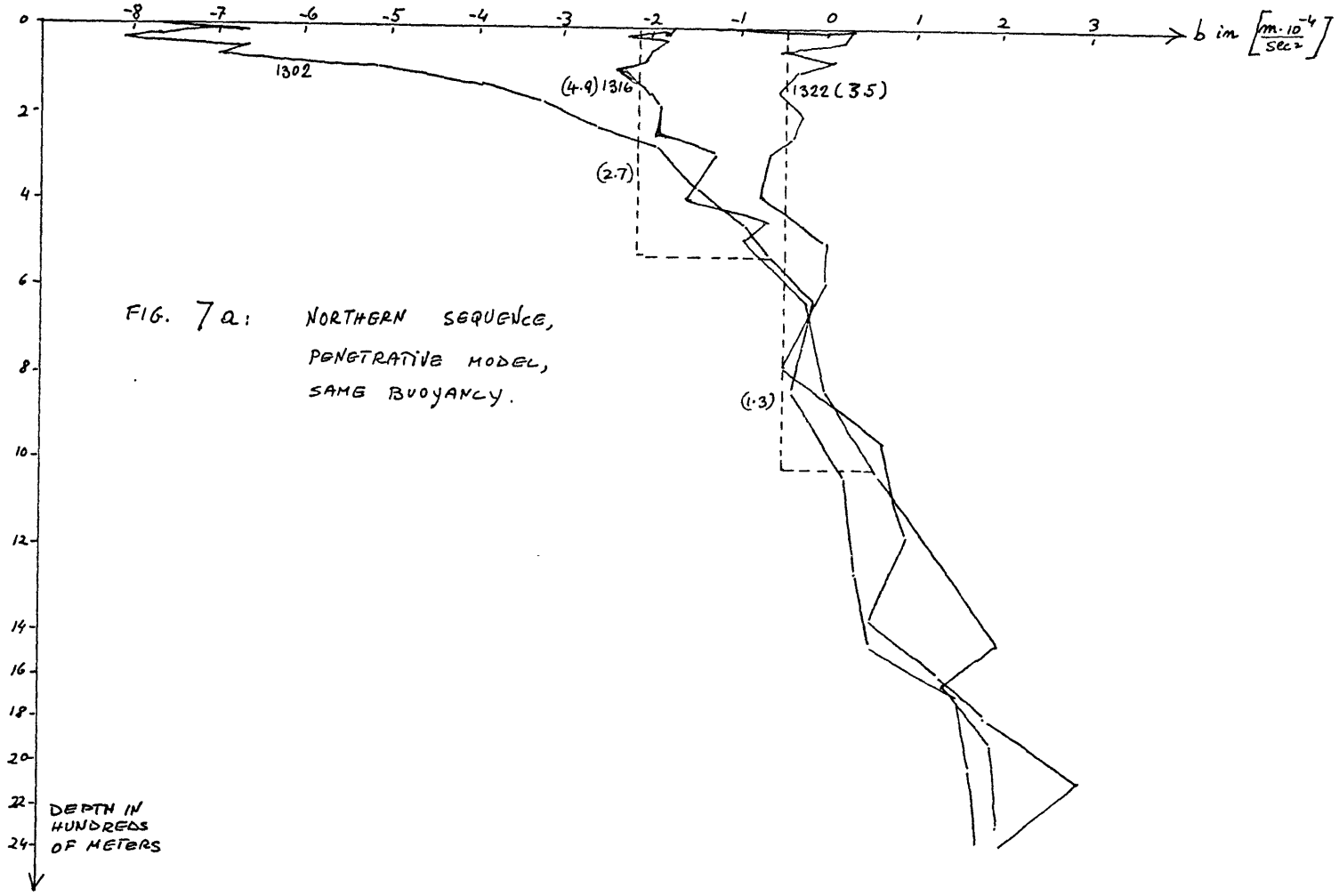

FIG. 7a: NORTHERN SEQUENCE, PENETRATIVE MODEL, SAME BUOYANCY.

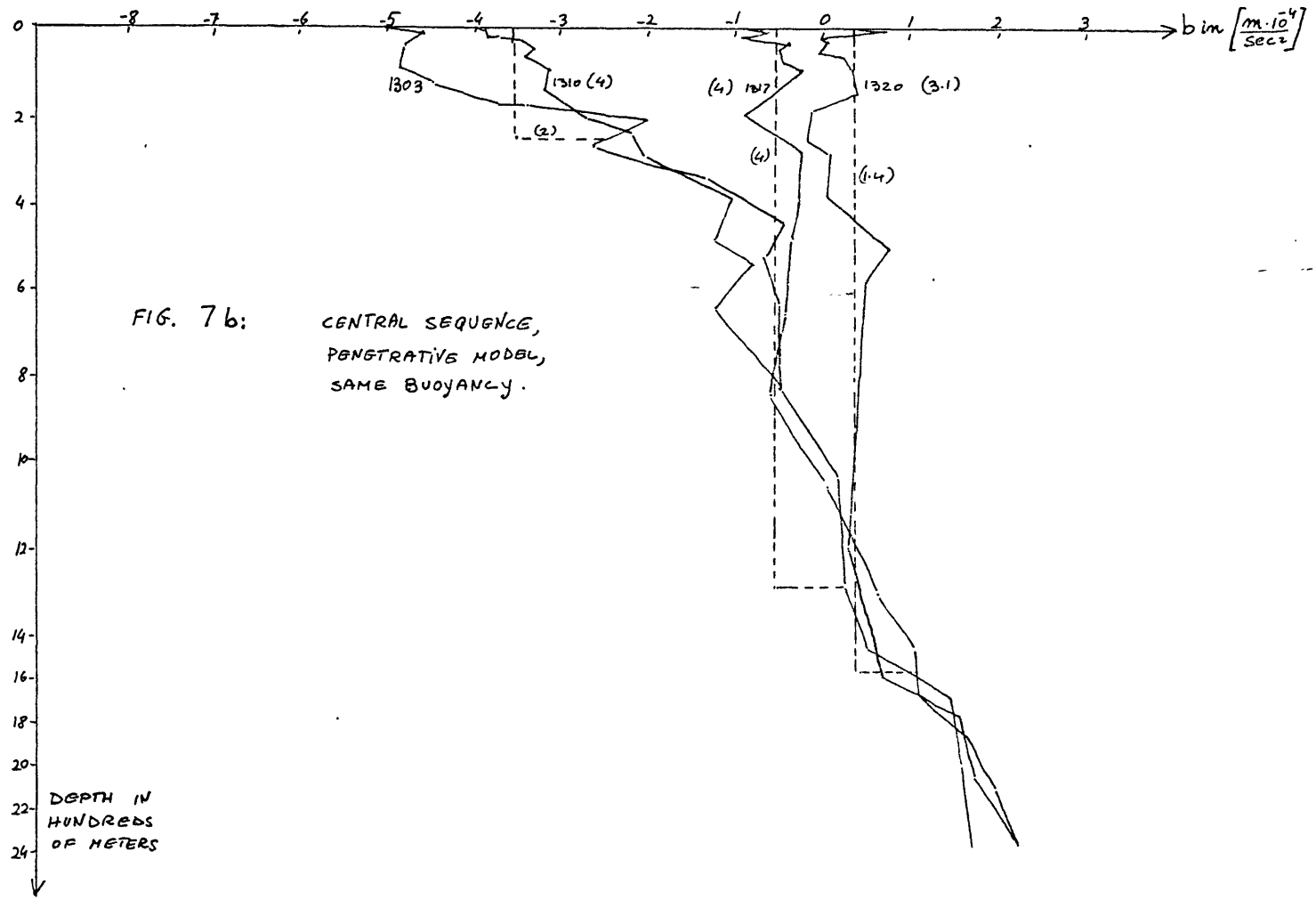

FIG. 7b: CENTRAL SEQUENCE, PENETRATIVE MODEL, SAME BUOYANCY.

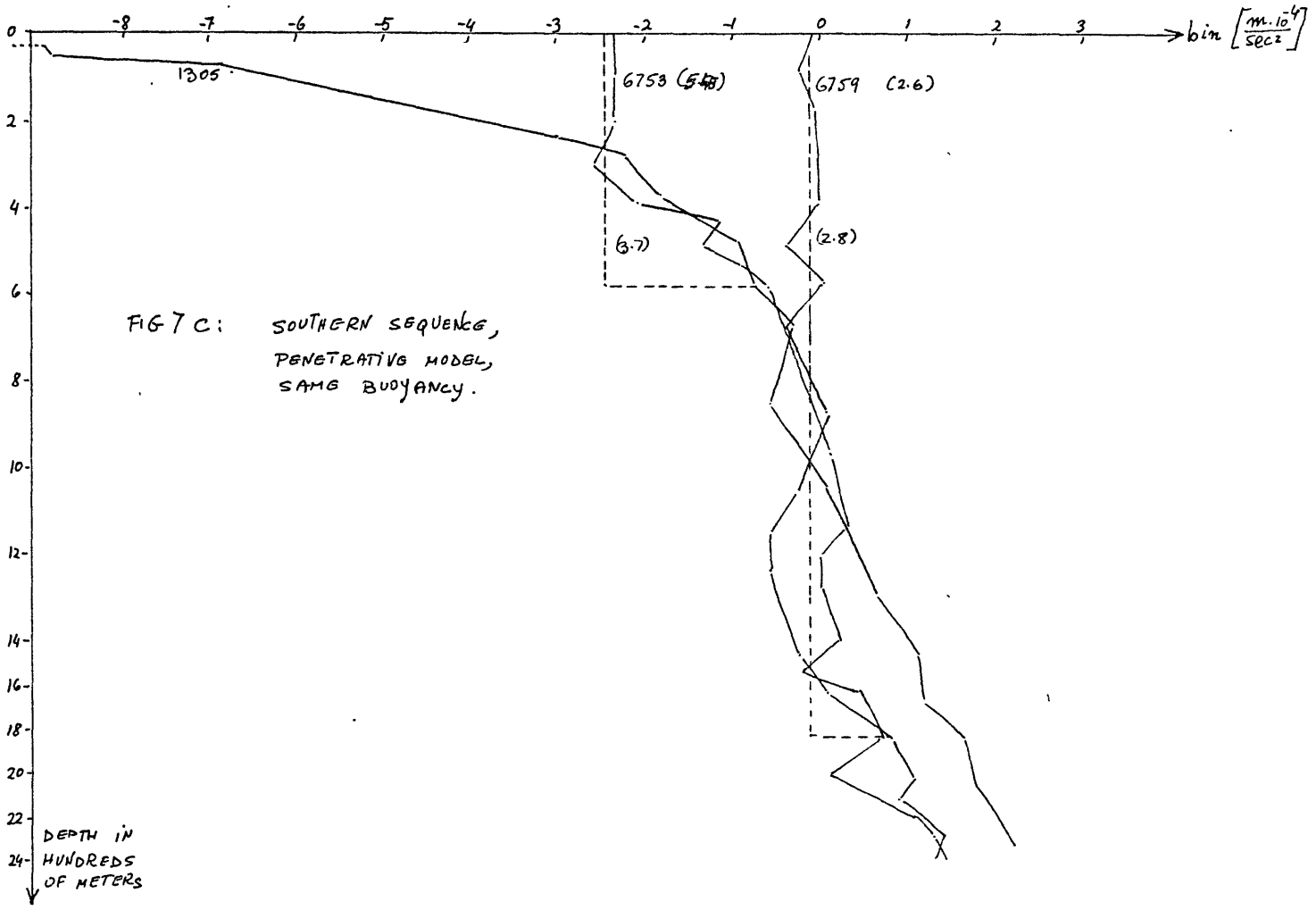

FIG 7 C: SOUTHERN SEQUENCE, PENETRATIVE MODEL, SAME BUOYANCY.

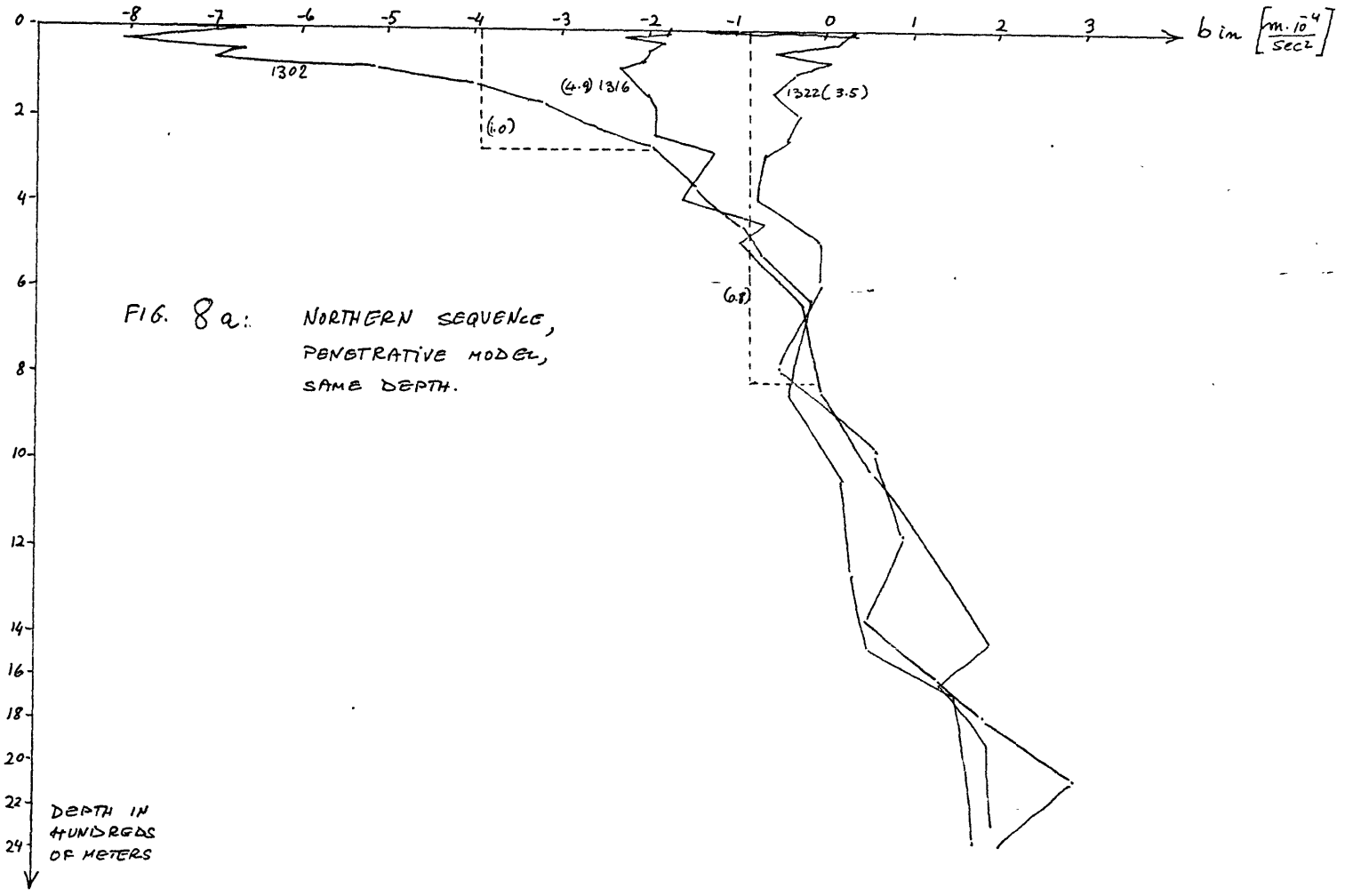

FIG. 8a: NORTHERN SEQUENCE, PENETRATIVE MODEL, SAME DEPTH.

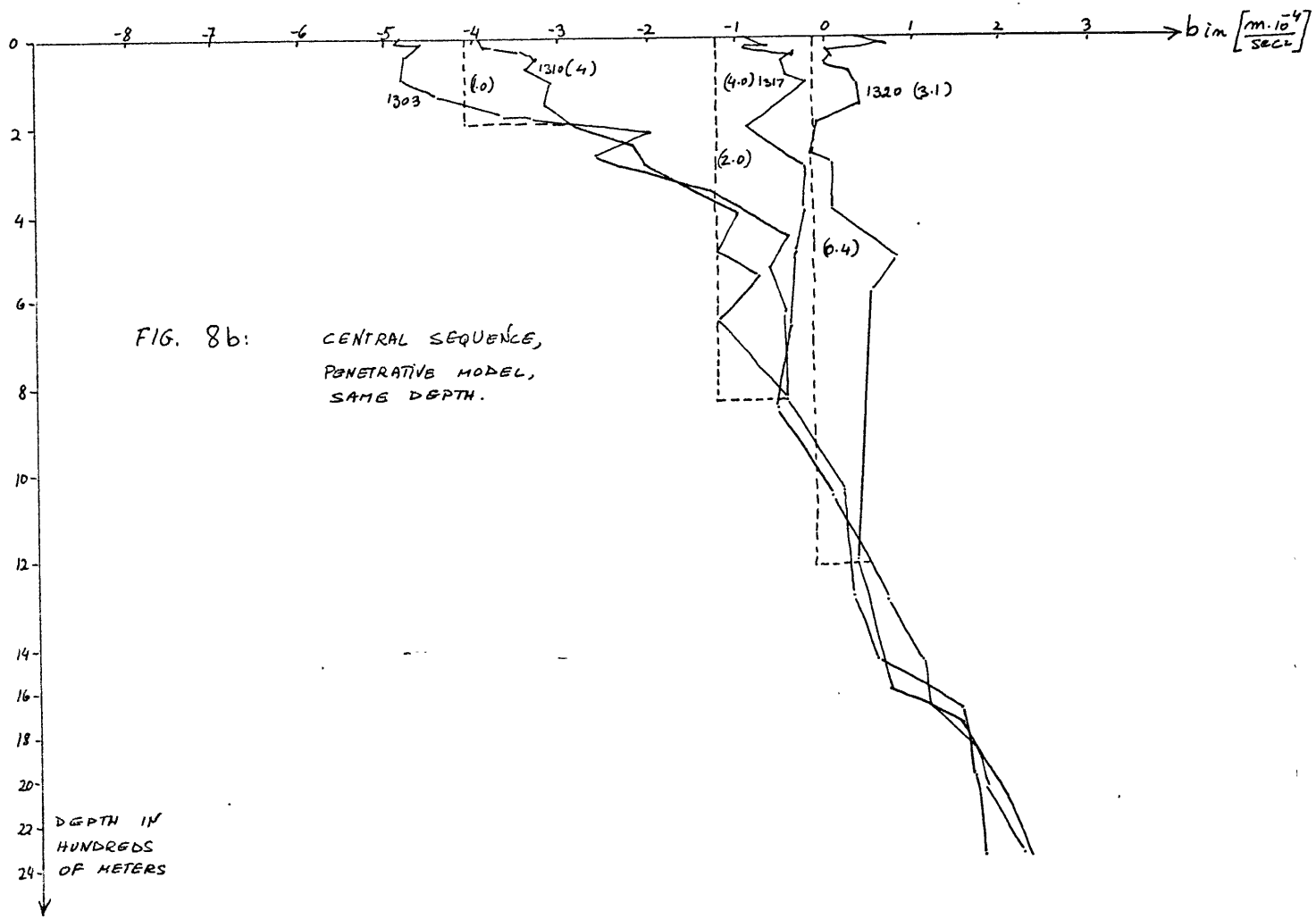

FIG. 8b: CENTRAL SEQUENCE, PENETRATIVE MODEL, SAME DEPTH.

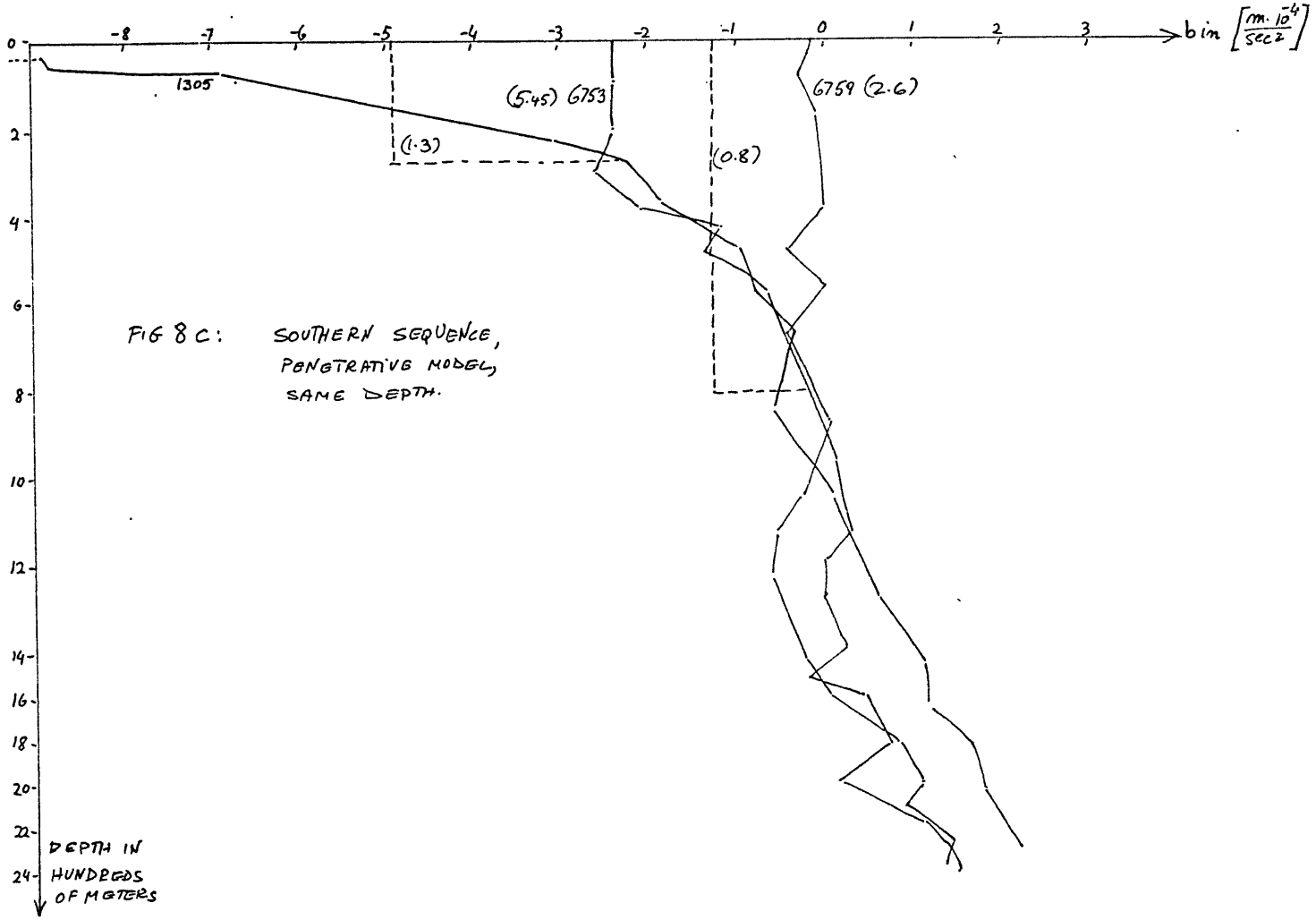

FIG 8C: SOUTHERN SEQUENCE, PENETRATIVE MODEL, SAME DEPTH.

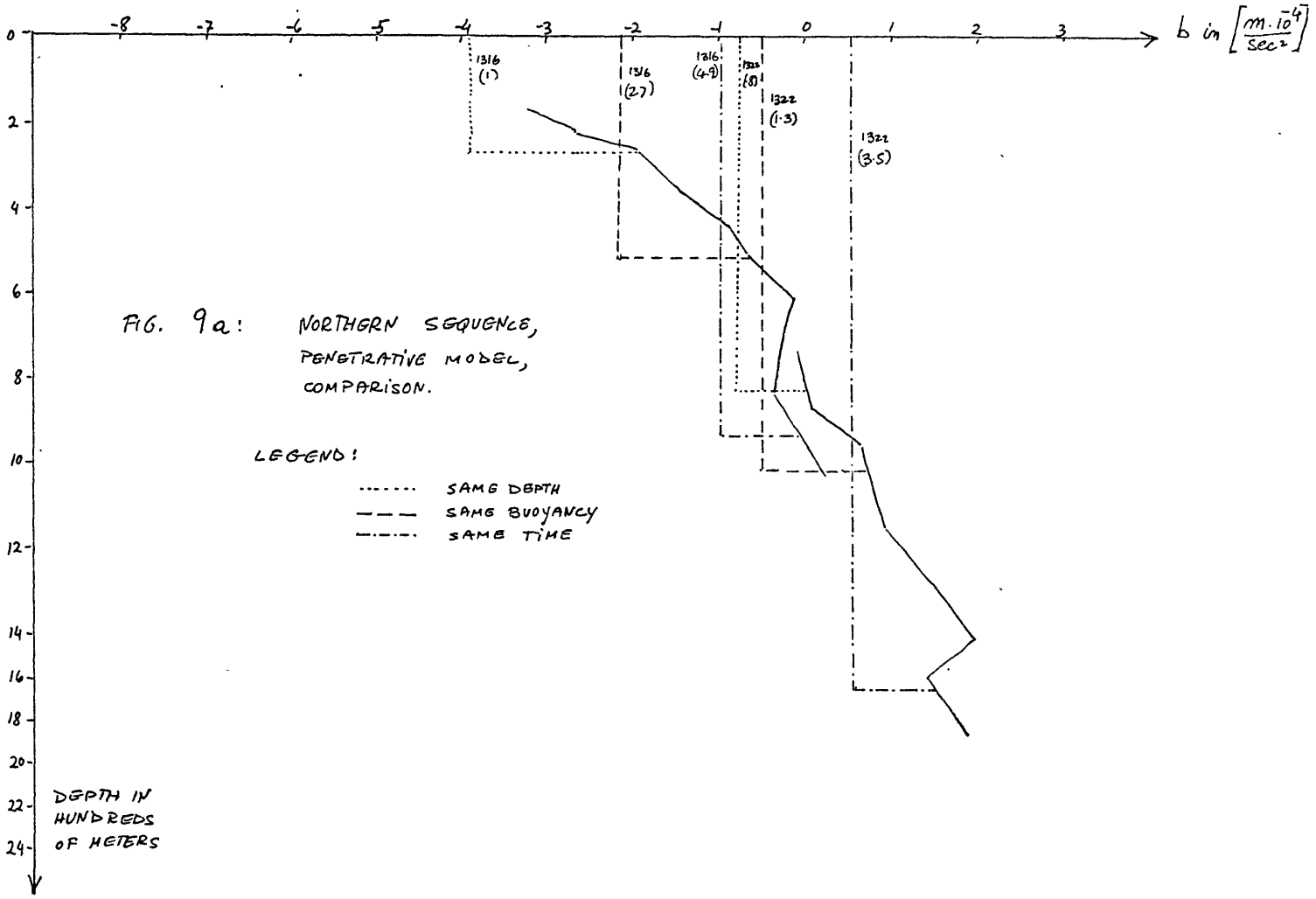

FIG. 9a: NORTHERN SEQUENCE, PENETRATIVE MODEL, COMPARISON.

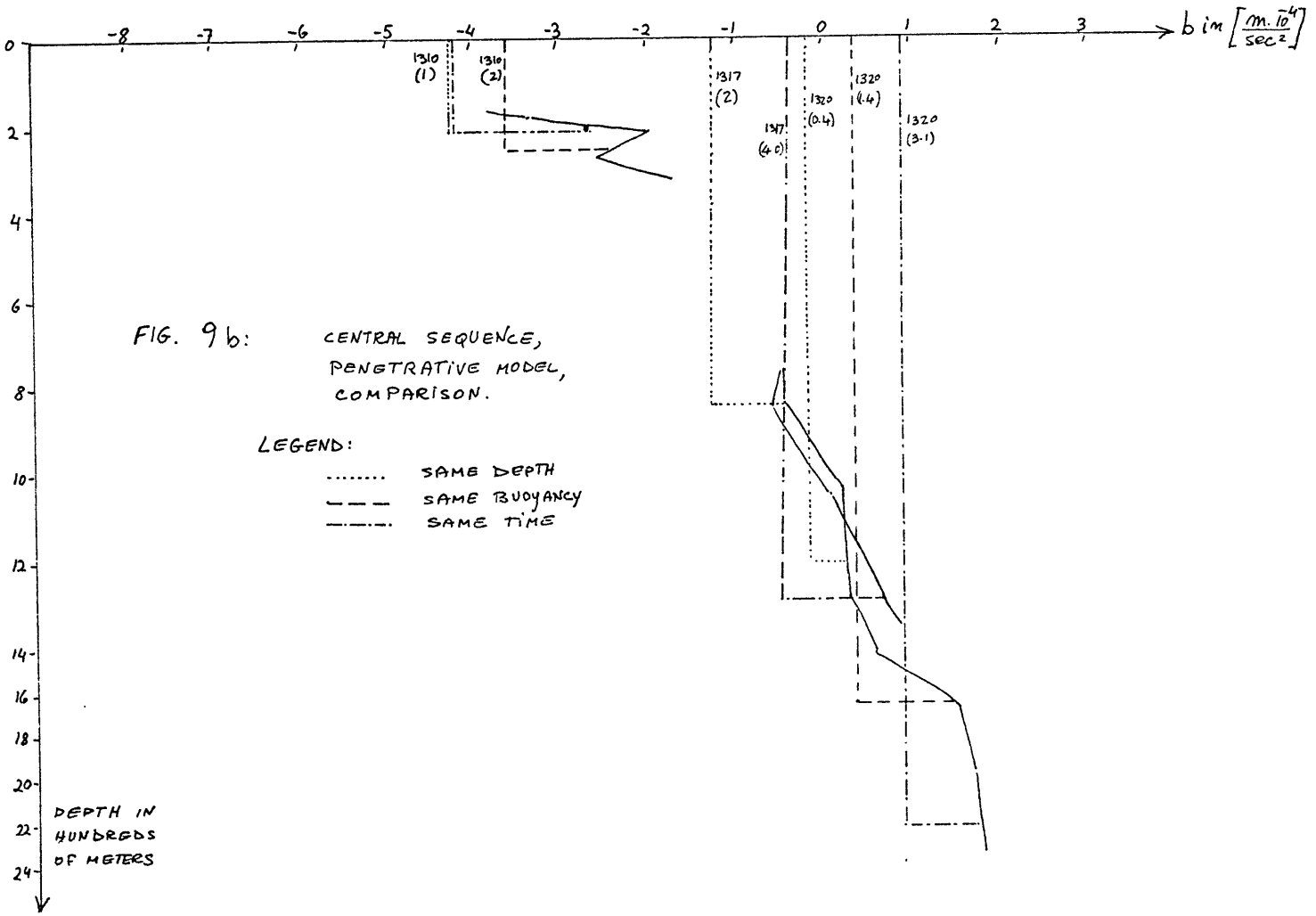

FIG. 9b: CENTRAL SEQUENCE, PENETRATIVE MODEL, COMPARISON.

LEGEND:

..... SAME DEPTH

– – – SAME BUOYANCY

–.–.– SAME TIME

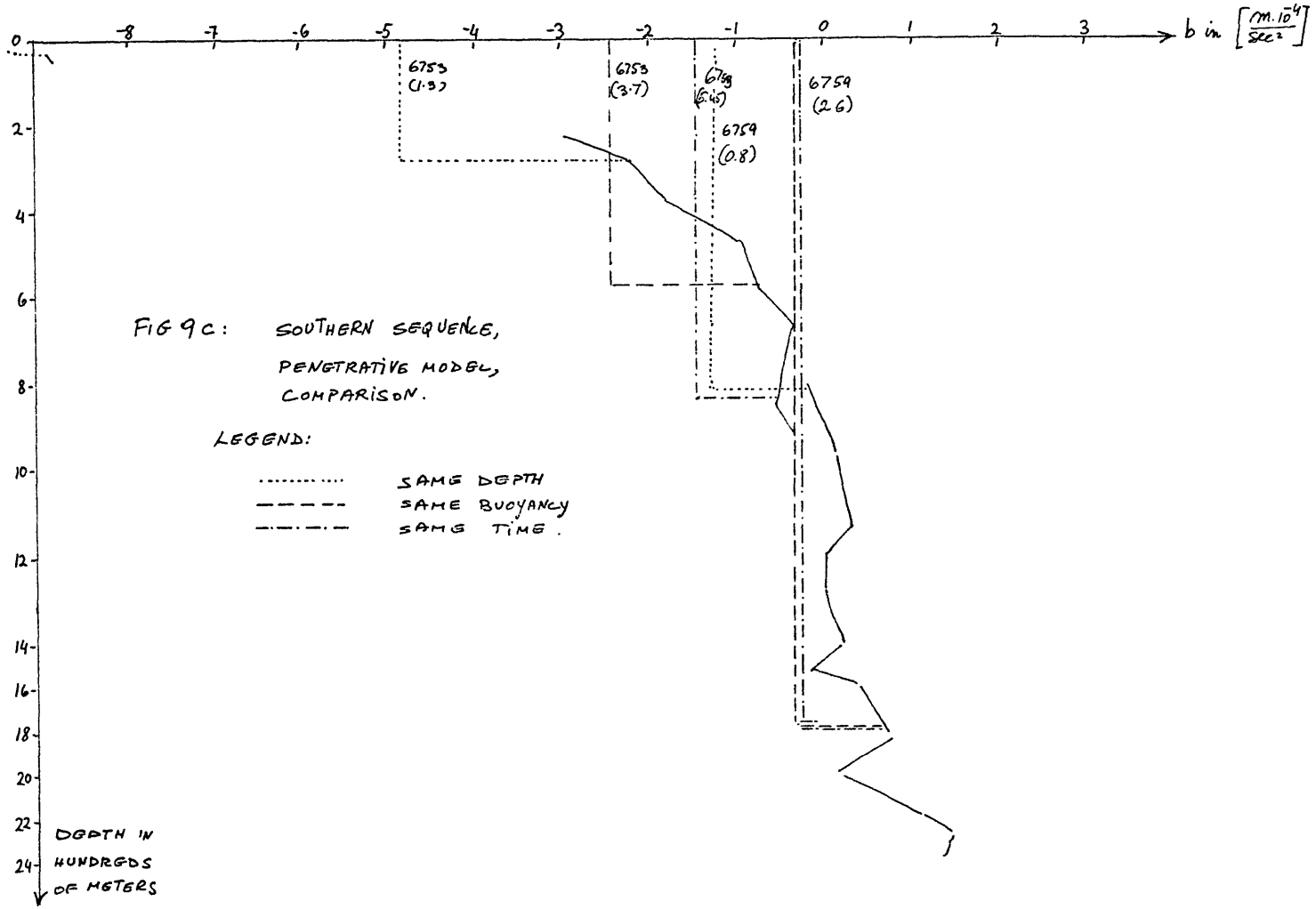
b in $\left[\frac{m.10^{-4}}{sec^2}\right]$
-8
-7
-6
-5
-4
-3
-2
-1
0
1
2
3
0
2
4
6
8
10
12
14
16
18
20
22
24
6753 (1.9)
6753 (3.7)
6758 (5.45)
6759 (0.8)
6759 (2.6)
FIG 9c: SOUTHERN SEQUENCE, PENETRATIVE MODEL, COMPARISON.
LEGEND:
SAME DEPTH
SAME BUOYANCY
SAME TIME.
DEPTH IN HUNDREDS OF METERS

COMPARING THE SEPARATE EFFECT OF E, H, AND W

Before we proceed with a non-penetrative model, we would like to check the relative importance of each of the three fluxes E, H, and W when acting separately.

For this purpose let's take station 1305, which is the most stably stratified among our stations, and operate our model with hypothetical conditions of E only, H only and W only.

It is worthwhile noting at this point that there are conflicting opinions among various authors as to the magnitude of the drag coefficient C_{DR}, as well as to its dependence on the wind speed.

For the purpose of this work Wu's formula was used in estimating the W and, following G. D. Robinson's recommendation for short-time measurements, the constant value $C_{DR} = 1.2 \times 10^{-3}$ was used in estimating the E and H. (See Appendix A.)

It is important to remember here that the effect of the latent heat of evaporation is included in the H and not in the E; E represents only the effect of evaporation on the surface salinity.

The results are shown in figure 10. What immediately emerges is that the effect of E is negligible. Thus, the increase in density due to increased salinity has a relatively small effect compared to the increase in density due to the cooling associated with evaporation. This is not unexpected. The second remarkable fact is that below 400 meters, the H alone and the combined E, H, and W are practically parallel to each other. This means of course that the effect of the

mechanical stirring can be noticeable only as long as the mixed layer is relatively shallow. Whatever turbulent entrainment is present below 400 meters is therefore mostly the indirect consequence of instabilities caused by the cooling of the surface.

In terms of average downward velocity, we have at a depth of two kilometers:

$$\text{E-effect} = 1.07 \sim 7\%$$

$$\text{H-effect} = 10.46 \sim 76\%$$

$$\text{W-effect} = 2.21 \sim 15\%$$

$$\text{Combined-effect} = 13.78 = 100\%$$

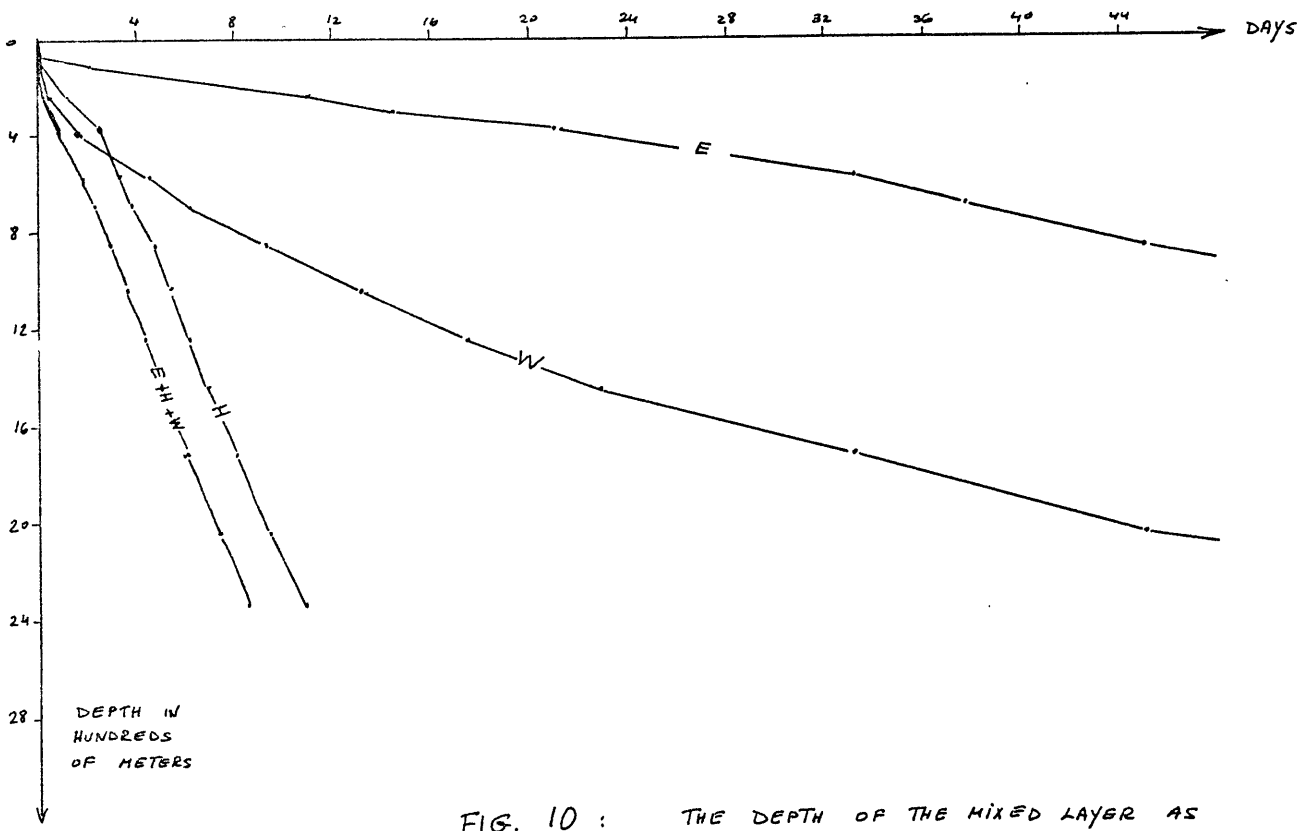

FIG. 10 : THE DEPTH OF THE MIXED LAYER AS A FUNCTION OF TIME FOR HYPOTHETICAL FLUXES.

THE NON-PENETRATIVE MODEL

We are now going to check the non-penetrative model and we take the same approach as for the previous case: we compare predicted profiles with observed ones. Figures 11a, 11b and 11c display the comparison using the same time as observed.

The general picture already seems to be more promising than that given by the penetrative model. When we compare the profiles taking the same depth or buoyancy as observed we are pleasantly surprised: within the accuracy expected, in all cases, with no exceptions, the two are indiscernable! Thus whenever we check the buoyancy predicted for a given depth, it turns out to be, as far as we can tell, exactly as the observed one, and vice versa: whenever we check the depth predicted for a given buoyancy it turns out to be, as far as we can tell, exactly as observed. In this case we therefore need only one set of diagrams that combines the two: figures 12a, 12b, and 12c.

To repeat the same criterion as in the previous case the profiles are displayed together on figures 13a, 13b, and 13c, and they definitely look more coherent than in the penetrative case.

We may safely deduce from these tests that the actual oceanic process is nearer to the non-penetrative model than to the penetrative.

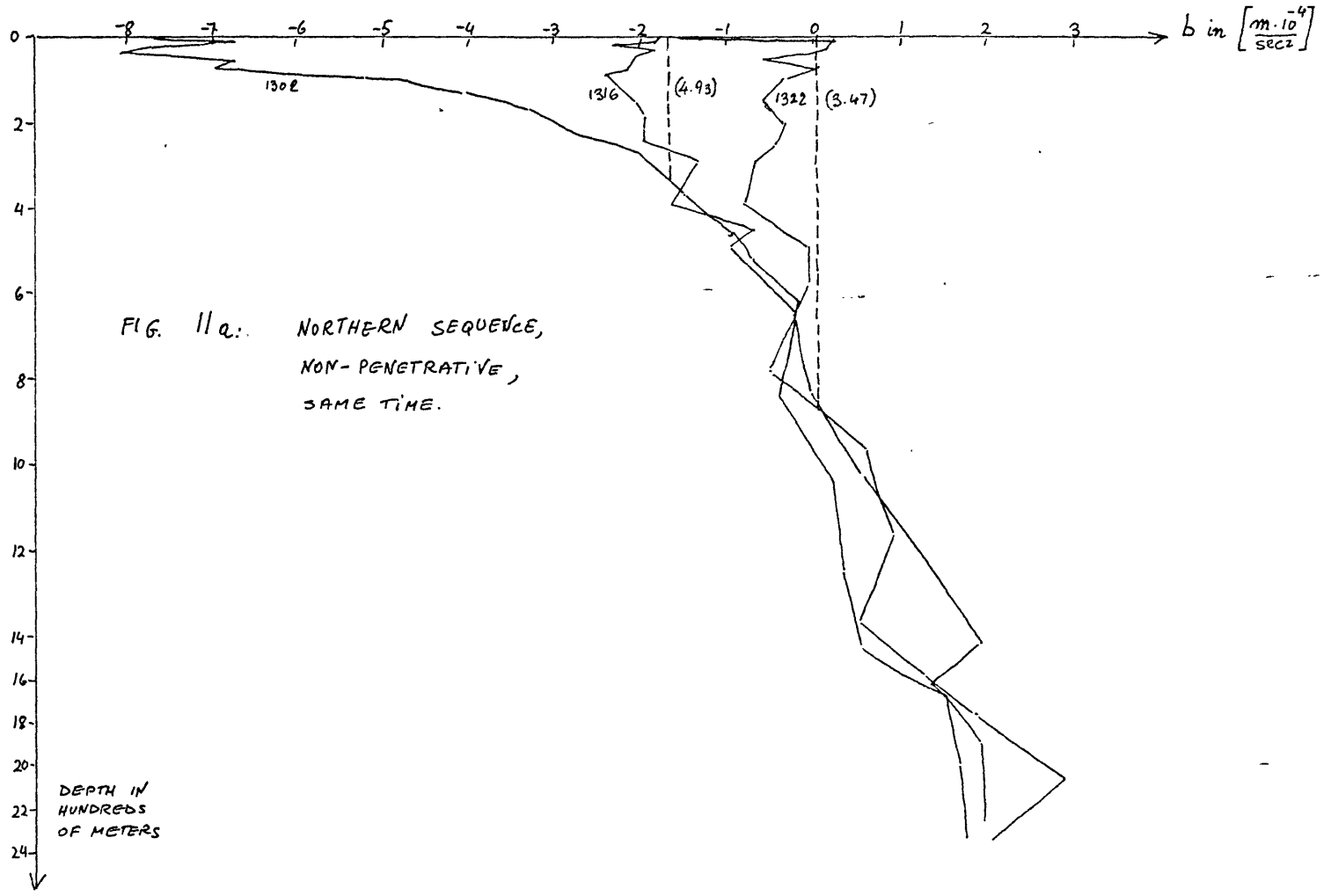

FIG. II a.: NORTHERN SEQUENCE, NON-PENETRATIVE, SAME TIME.

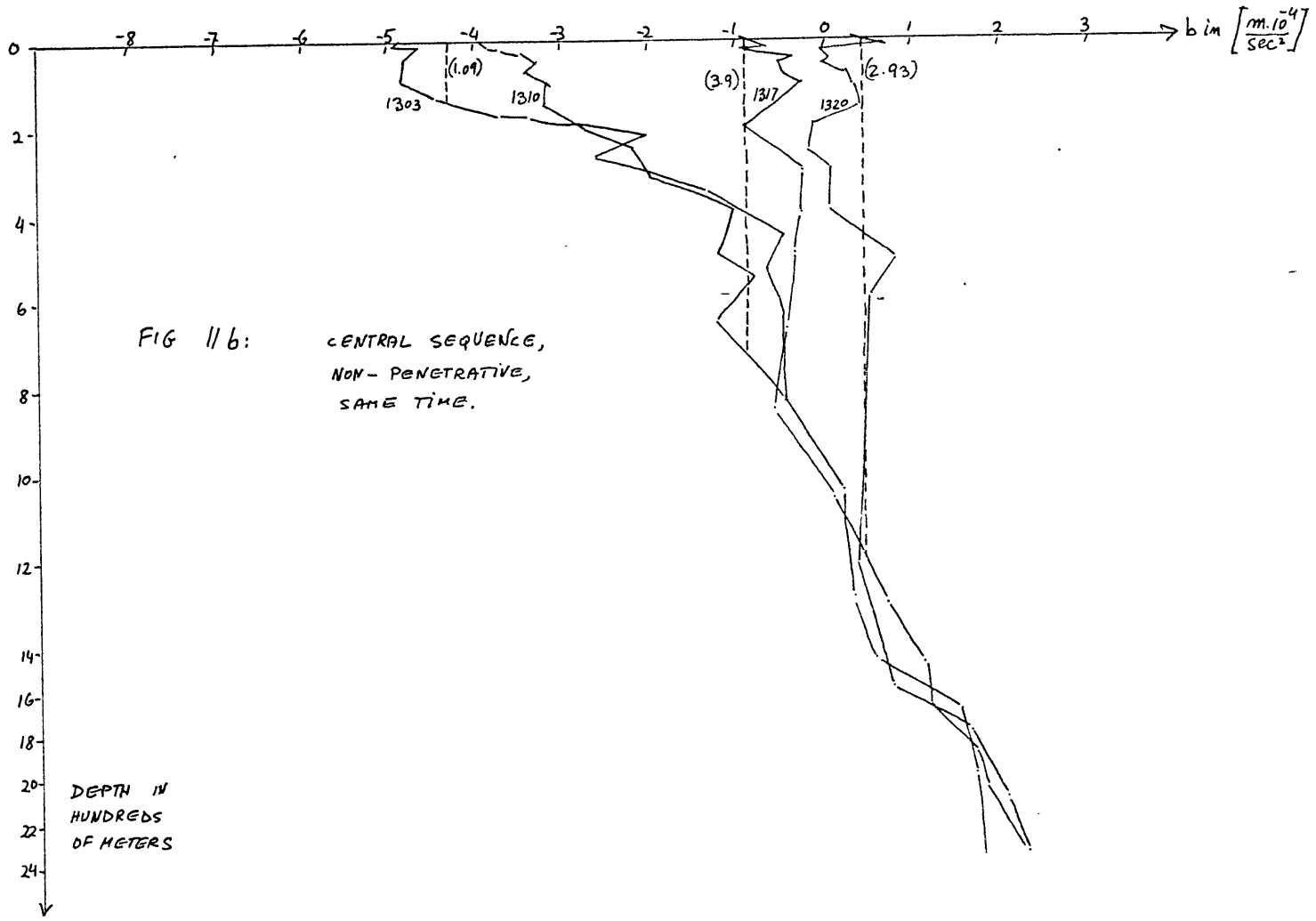

FIG II 6: CENTRAL SEQUENCE, NON-PENETRATIVE, SAME TIME.

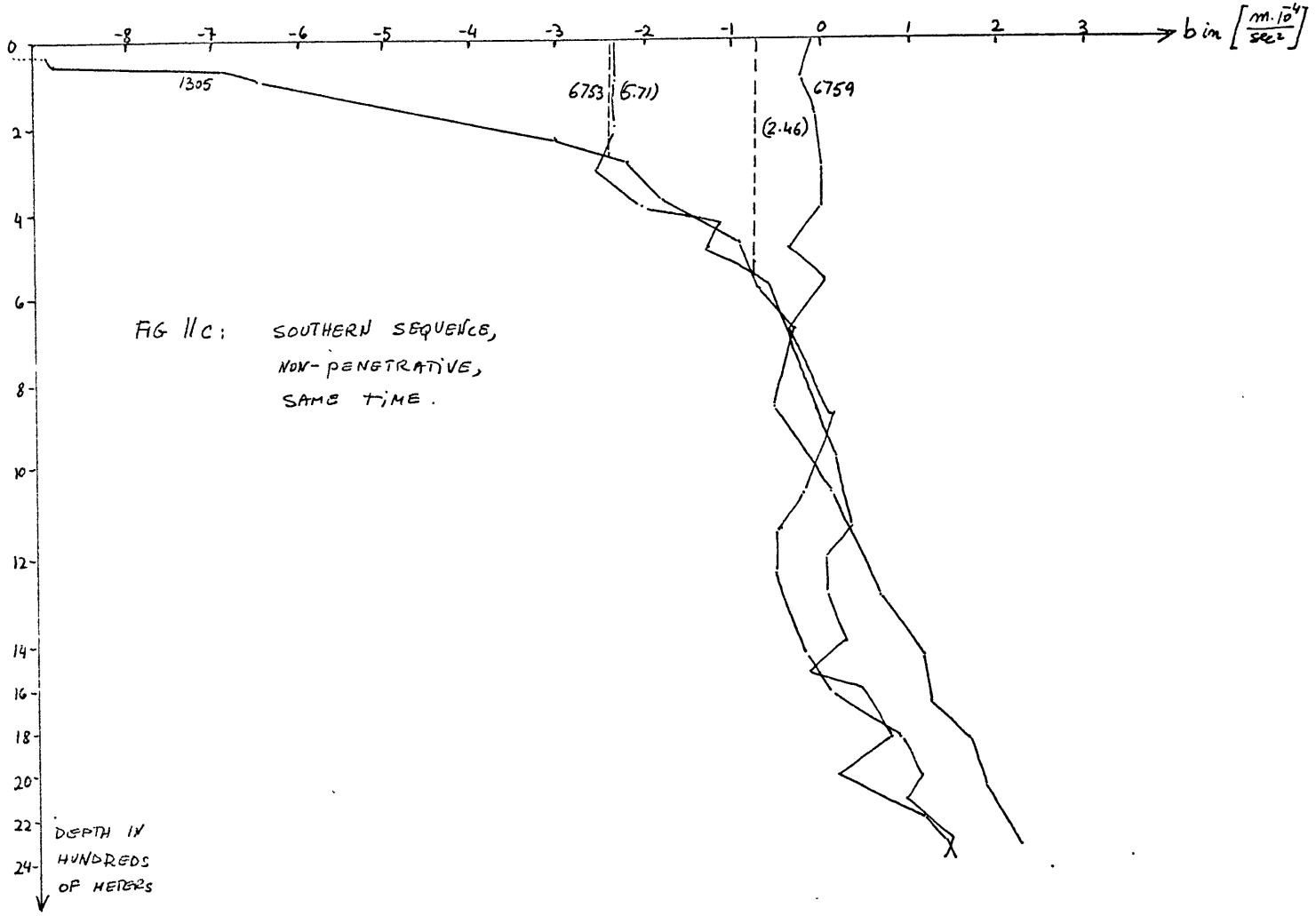

FIG II C: SOUTHERN SEQUENCE, NON-PENETRATIVE, SAME TIME.

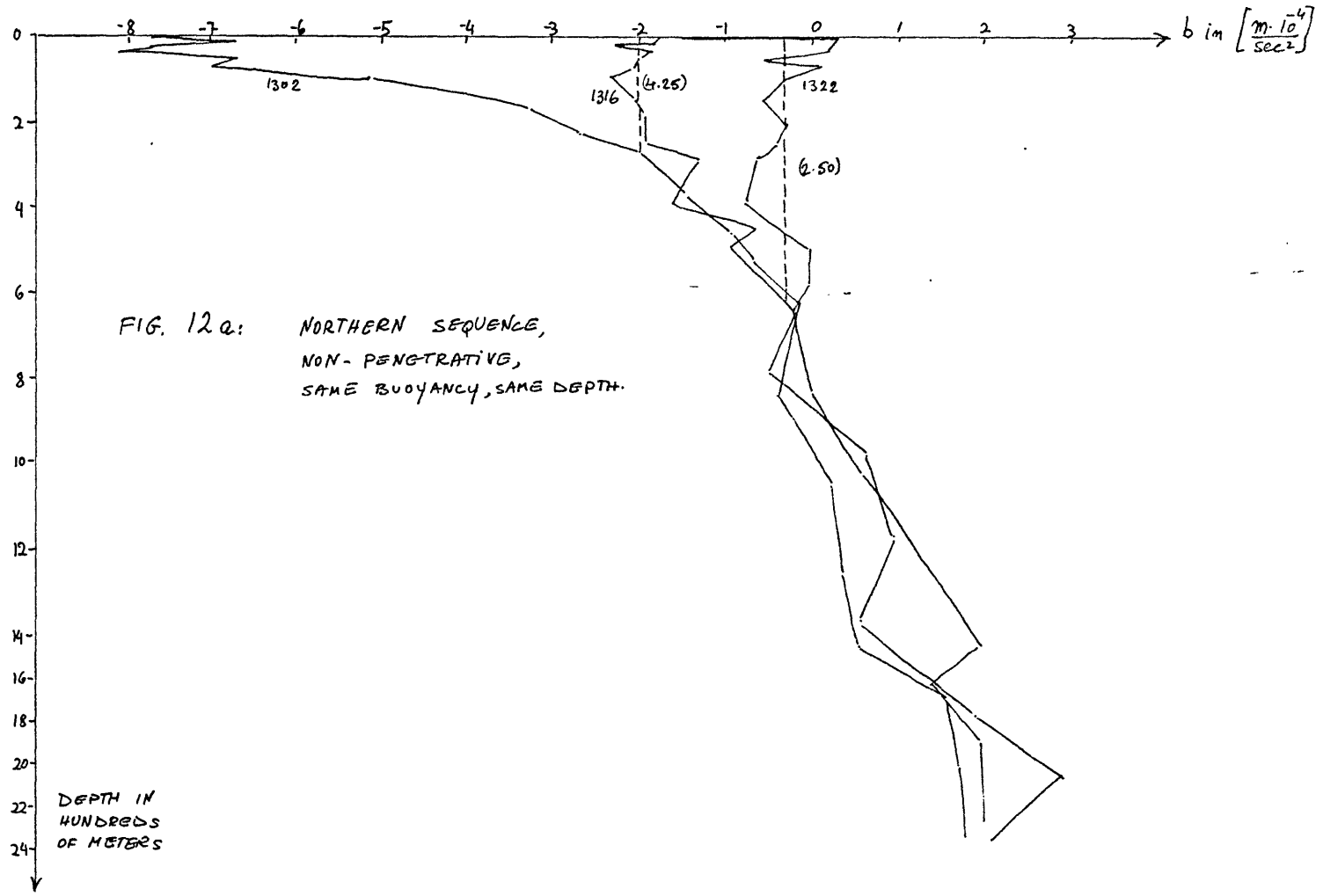

FIG. 12a: NORTHERN SEQUENCE, NON-PENETRATIVE, SAME BUOYANCY, SAME DEPTH.

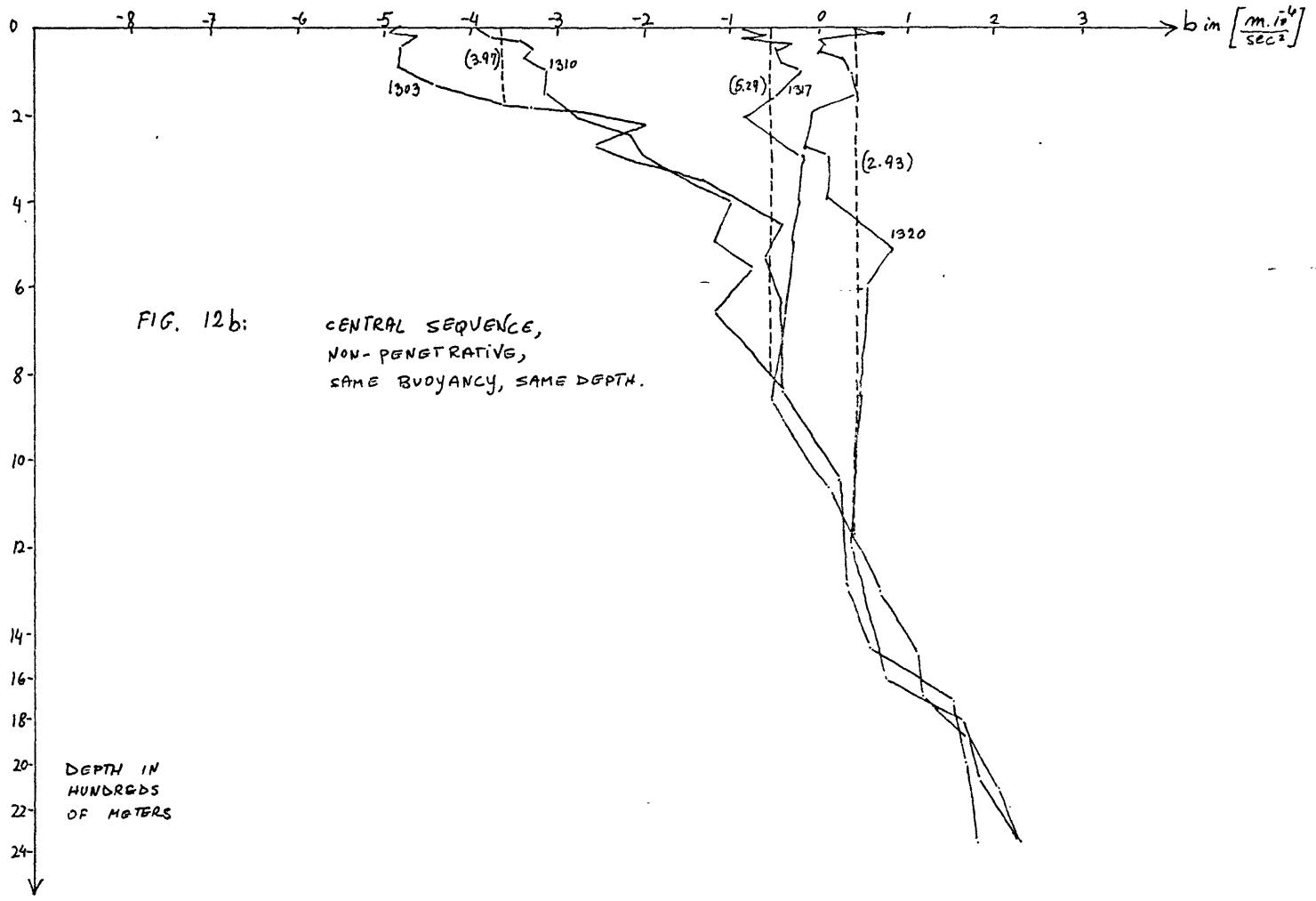

FIG. 12b: CENTRAL SEQUENCE, NON-PENETRATIVE, SAME BUOYANCY, SAME DEPTH.

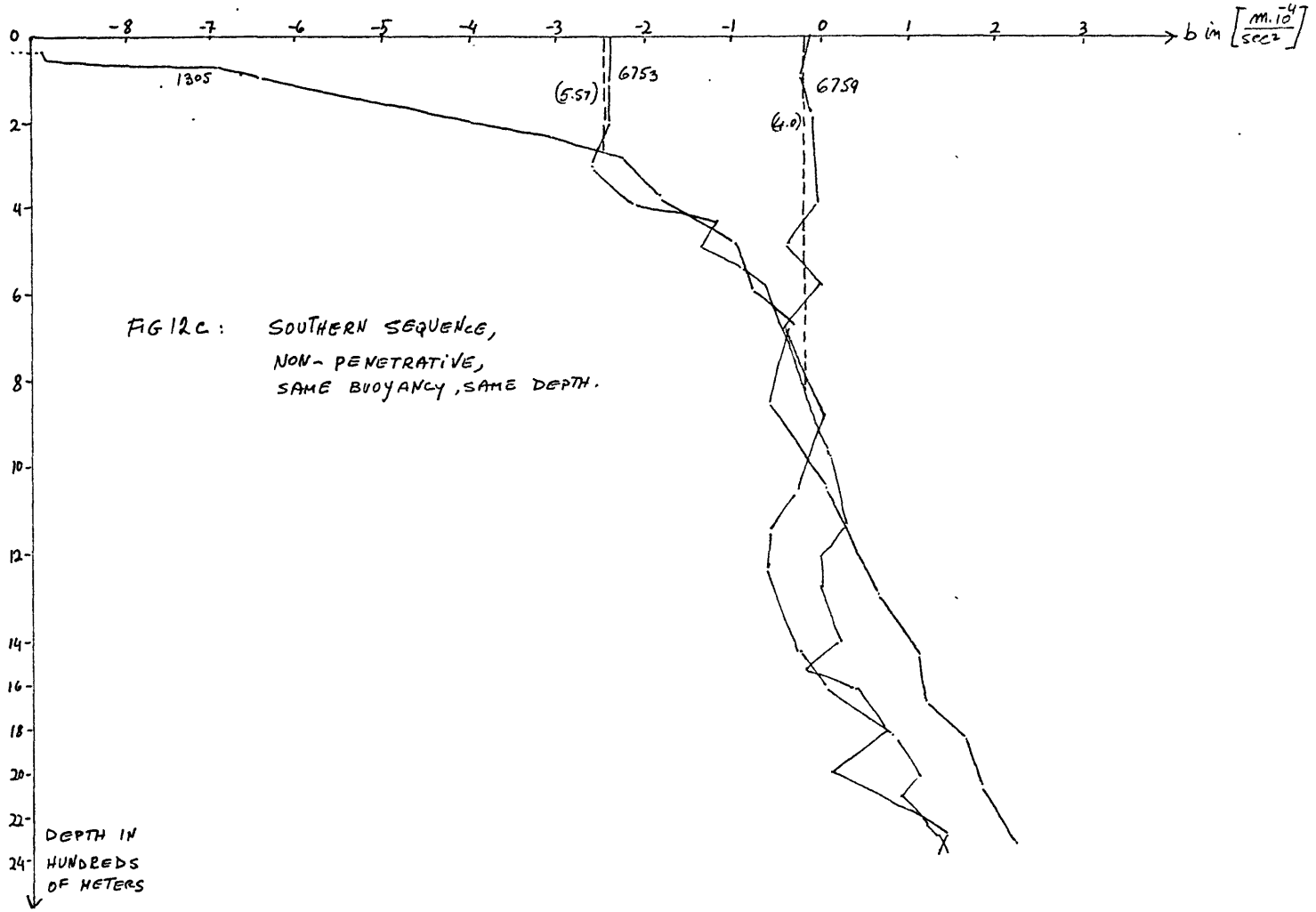

FIG 12c: SOUTHERN SEQUENCE,
NON-PENETRATIVE,
SAME BUOYANCY, SAME DEPTH.

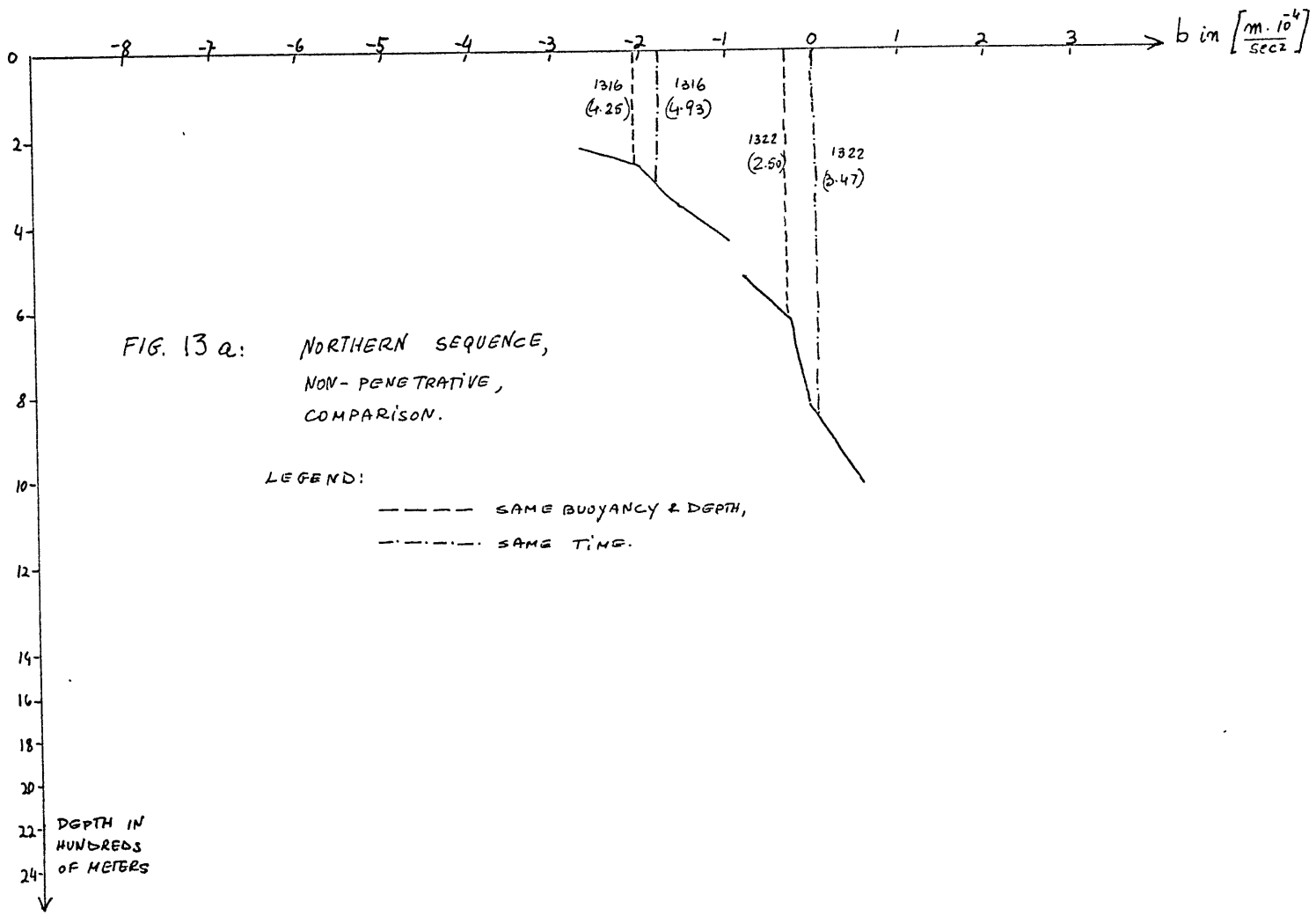

FIG. 13 a: NORTHERN SEQUENCE, NON-PENETRATIVE, COMPARISON.

LEGEND:

——— SAME BUOYANCY & DEPTH,

—·—·— SAME TIME.

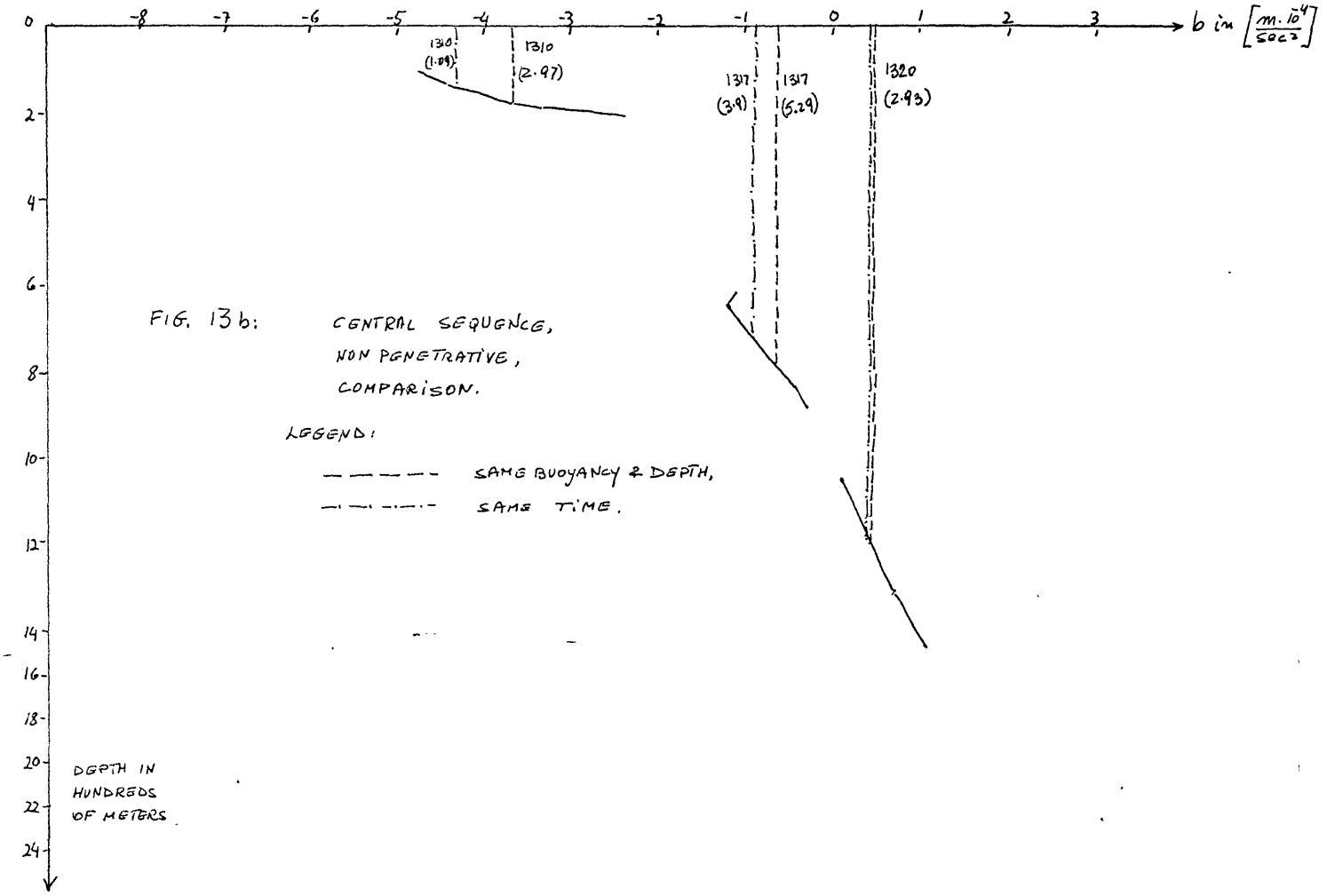

FIG. 13b: CENTRAL SEQUENCE, NON PENETRATIVE, COMPARISON.

LEGEND:

— — — — — SAME BUOYANCY & DEPTH,

— · — · — · — SAME TIME.

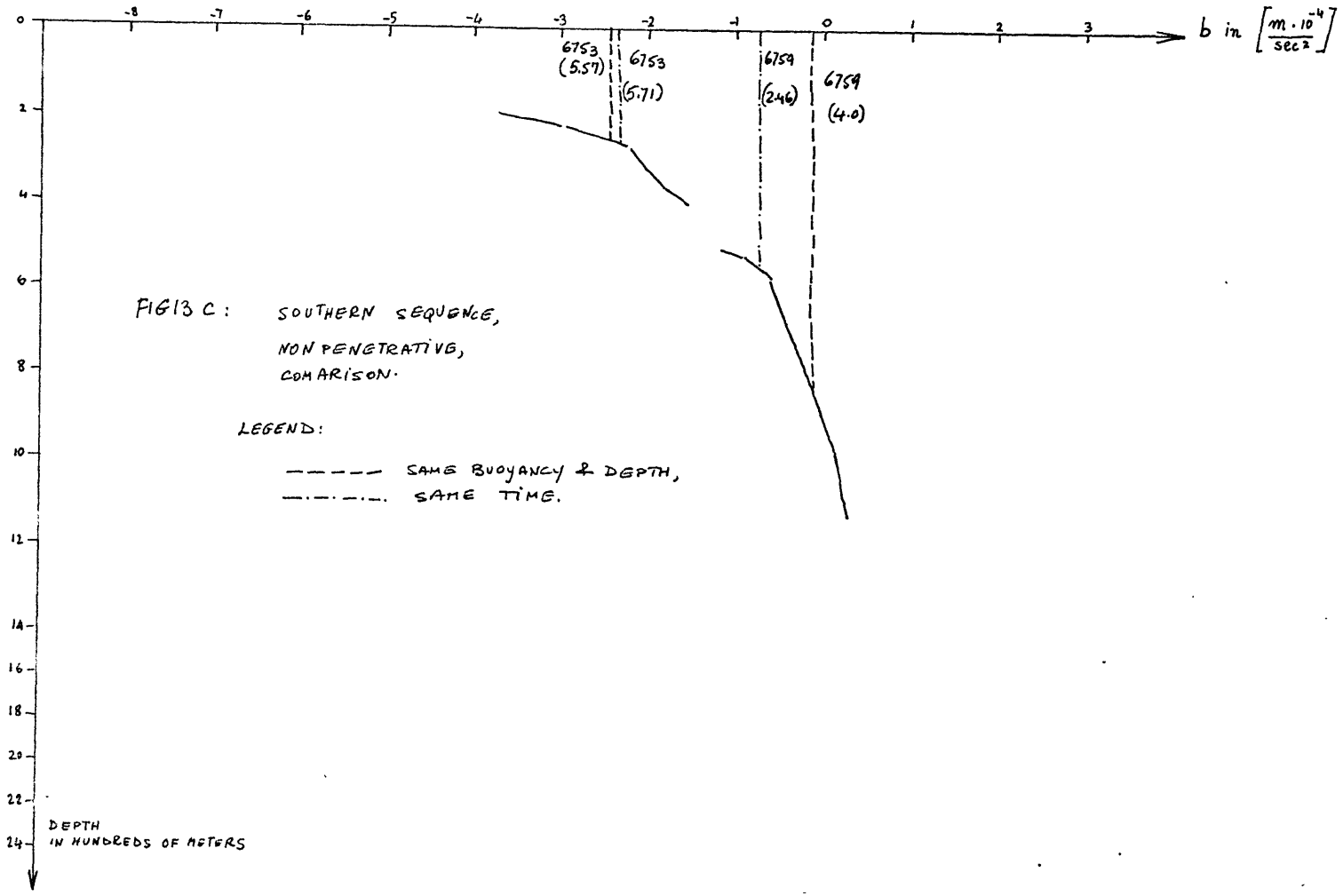

FIG13 C: SOUTHERN SEQUENCE, NON PENETRATIVG, COMARISON.

CHECKING VALIDITY OF ONE-DIMENSIONAL MODELS

As pointed out in the second chapter, all models so far were one-dimensional models, which is equivalent to assuming that each column of oceanic water interacts with the atmosphere separately, but that adjacent columns do not interact with each other.

None of the authors of the various models tried very hard to justify this assumption. First of all it seems the natural first step in trying to solve this problem, since it is the simplest model. Second, generally speaking the horizontal gradients commonly found in oceanic situations are so small compared to vertical gradients that one is naturally inclined to think that lateral processes are relatively unimportant.

In this case, however, a mere look at the typical sections shown by Anati and Stommel (1970) convince us that there is reason to doubt the validity of such an approach for this particular case.

Now we are going to make a rough test on this assumption in the following way: We define for each pair of stations a dimensionless quantity t* as the ratio of the time required according to our non-penetrative model to reach the observed depth (and observed buoyancy) to the time observed to have actually lapsed between the two stations.

$$t^* \equiv \frac{\text{time required}}{\text{time observed}}$$

Whenever $t^* > 1$ we understand that the observed deepening of the mixed layer and the accompanying increase in buoyancy is more advanced than predicted. Whenever $t^* < 1$, the observed deepening of the mixed layer and the accompanying increase in buoyancy is less advanced than predicted.

In order to make the picture clearer we display these numbers, between the stations, and in the proper sequences:

North:	1302		t*=0.86		1316	t*=0.72	1322
Center:	1303	t*=2.72	1310	t*=1.36	1317	t*=1	1320
South:	1305		t*=0.97		6753	t*=1.63	6759

We already pointed out that station 6759 is expected to be in a more advanced state than predicted, and indeed it's t^* is 1.63. With this exception, all other t^* show a remarkable fact: the center of the mixed layer deepens more rapidly than a one-dimensional model would predict, the adjacent columns deepen more slowly. To use everyday language: the center deepens more, at the expense of adjacent waters! This seems to indicate that neighboring columns of water do interact with each other and that at least a two-dimensional model will be required if we want to have any appreciable improvement on our present understanding of this important process.

It is interesting to note that the average t^* is

$$\overline{t^*} = 1.32 \ .$$

Of course, we don't know how far apart the sequences have to be in order to have equal weight in the averaging, or even if the sequences have to be parallel rather than, say, diverging. But just to make a rough test on our flux estimates, we may note that if station 6759 were more suitably located, we could have been rather close to the ideal flux-estimates of

$$\overline{t^*} = 1 \ .$$

Just for curiosity let's compare these t*'s with the t*'s for the penetrative model:

1302		t*=4.9		1316	t*=4.4	1322
1303	t*=4.0	1310	t*=2.0	1317	t*=7.6	1320
1305		t*=4.2		6753	t*=3.8	6759

with $\overline{t^*} = 4.41$.

CONCLUSIONS

The penetrative and non-penetrative models are extreme cases, idealized so to speak, and although the penetrative one appears *a priori* to be a plausible one, we really do not expect either case to apply exactly: we did not expect the cooling of the water not to effect the potential energy at all, and we did not expect an entirely non-turbulent process to occur during the blowing of the mistral, but rather somewhere between these two. All we can say is that evidence for this particular region and this particular season seems to favour one model, the non-penetrative one, more than the other. Some entrainment must occur during such violent mixing but according to the stations chosen for the present work this entrainment seems negligible.

It is worth noting that Stommel arrived at similar conclusions about penetrative versus non-penetrative models (Stommel, 1970) using entirely different methods.

If we adopt the non-penetrative model one important point remains still to be cleared: this model ignores entirely the effect of the W, but on the other hand we saw that for the first hundreds of meters the W-effect cannot be neglected, in fact it seems to be the principal contributor to the deepening of the mixed layer. The clue to this apparent conflict seems to lie in one wrong assumption: As we pointed out on page 22 all of the W-energy flux was assumed to be converted into potential energy through entrainment and with this assumption the W-effect turned out indeed to be important in the

first hundreds of meters. If on the other hand most of this energy were going into current generation, or wave generation radiated away, or even dissipated, then the entrainment could be negligible even at depths less 400 meters. Since mechanical mixing certainly occurs at the very surface, it still remains to be seen to what depth this process is still noticeable. All we can say for the time being is that for all depths checked within the frame of this work, this process was entirely overshadowed by the cooling effect.

Referring now to the fact that $\overline{t^*} \sim 1$, we may also point out that as a by-product of our comparisons, we gained some more confidence in the flux estimates than depicted on page 23.

Another conclusion we must draw from our results is that we need a two-dimensional model to explain this phenomenon. The difficulty in formulating any tentative two-dimensional model is our lack of knowledge about lateral effective diffusivity or rather "diffusivities" in plural, since we do not know a priori whether or not in spite of the obvious turbulent state, we can take Prandtl number = Schmidt number = 1. In view of the unexpectedly small effect the turbulence seems to have on the entrainment at the bottom of the mixed layer, it would be wise to be very cautious.

REFERENCES

Anati, D. and H. Stommel, 1970: The initial phase of deep water formation in the Northwest Mediterranean, during Medoc '69, on the basis of observations made by "ATLANTIS II". Cahiers Océanographiques, XXIIe Année, No. 4, 343-352.

Ball, F., 1960: Control of inversion height by surface heating. Q. J. Roy. Met. Soc. 86, 483-494.

Cromwell, T., 1960: Pycnoclines created by mixing in an aquarium tank. J. Mar. Res., 18, 78-82.

Francis, J. and H. Stommel, 1953: How much does a gale mix the surface layers of the ocean? Q. J. Roy. Met. Soc. 79, 534-536.

Kato, H. and O. M. Phillips, 1969: On the penetration of a turbulent layer into stratified fluid, J. F. M. 37, 643-655.

Kraus, E. and C. Rooth, 1961: Temperature and steady state vertical heat flux in the ocean surface layers. Tellus, 13, 231-238.

MEDOC Group Report, 1970, in press.

Rossby, C.g. and R. B. Montgomery, 1935: The layer of frictional influence in wind and ocean currents. Papers in Phys. Oc. and Met., 3, No. 3, 1-101.

Stommel, H, 1970: in press.

Tabata, S., Boston, N. and F. Boyce, 1965: The relation between wind speed and summer isothermal surface layer of water at Ocean Station P in the Eastern Subarctic Pacific Ocean. J. Geo. Res., 70, 3867.

Turner, S. and E. Kraus, 1965: A one-dimensional model of the seasonal thermocline, I and II. Tellus, 19, 88-105.

APPENDIX A

AIR-SEA INTERACTION PROGRAM

INPUTS:	TA = Air temperature at deck (mast) height	Deg. C°
	TS = Sea surface temperature	Deg. C°
	TW = Wet-bulb temperature	Deg. C°
	IU = Wind speed	Kts.
	IC = Cloudiness	Octans
	P = Atmospheric pressure	mb.
	RH = Relative humidity	%/100
	S = Insolation	cal/cm^2min
	ID = Wind direction	tens of degrees
	JH, J, M, IY = Hour local, day, month, & year	
	PHI, GAMMA = Latitude and Longitude	(+) for N & E (-) for S & W
OUTPUTS:	CDR = Drag coefficient	10^3
	# ESA, EA, EO = Vapour pressures	mb.
	* E = Evaporation rate	TMS. 10^9
	# TRP = Atmospheric transmittancy	%
	# ALB = Sea surface albedo	%
	# RB = Back radiation	TMS. 10^3
	RNH = Net heat loss by back radiation	TMS. 10^3
	* QE = Heat loss by evaporation	TMS. 10^3
	* QS = Heat loss by sensible heat transfer	TMS. 10^3

* H	= QE + QS + RNH	TMS. 10^3
W	= Mechanical energy input by wind stirring	TMS. 10^6
TAU	= Wind stress	TMS. 10^6
TRAN	= Ekman's transport	TMS

\# These values are auxiliary, and not printed out in the present form.

* These values are labeled 1 if computed with CDR being a function of wind speed [3], [4], or labeled 2 if computed with CDR = Const. = 1.2×10^{-3} [2]. Only those labeled 2 are printed out in the present form.

TIMES & UNITS: The program is planned to give a series of output values, OUP(N), as a function of a series of input values, at given times. For convenience and as customary in meteorology, the times are: 00, 06, 12, 18 local time; i.e., 4 times a day.

The program is aimed to give the outputs in the Ton-Meter-Second units, (TMS). The energy unit is therefore the Kilojoule.

For display purposes, the output values have been multiplied each by a convenient power of 10.

CDR: The drag coefficient CDR is computed according to Wu's formula [4], where UA = wind speed in m/sec.

$$CDR = \begin{cases} .5 \times 10^{-3} & UA < 1 \\ .5 \times \sqrt{UA} \times 10^{-3} & 1 \leq UA \leq 14.5 \\ 2.6 \times 10^{-3} & 14.5 < UA \end{cases}$$

E: $E = \rho_a \cdot C_{DE} \cdot \Delta q \cdot UA$ [1], [2], where ρ_a is taken as constant = 1.22×10^{-3} tons/m^3. Δq is taken as follows:

(i) Saturation vapour pressures ESA and ESO are computed for TA and TS, using the Goff-Gratch formula [5]. (Smithsonian tables [9], erroneous in this formula).

(ii) ESA is multiplied by the relative humidity RH to give EA.

(iii) A defined function computes the specific humidity from the P, and EA (or ESO):

$$q = \frac{0.622\ EA}{P - 0.378\ EA} \qquad [6]$$

(iv) Δq is the difference between the two.

TRP: The transmissivity of the atmosphere to back radiation is taken according to Berliand's formula [7]. As quoted by N. Clark [8]:

$$TRP = 0.97\left[\left(0.39 - 0.05\sqrt{EA}\right)\left(1 - FC \cdot 1C^2\right) + 4\left(1 - \frac{TA}{TS + 273.16}\right)\right]$$

The factor FC is taken to vary with latitude as:

$$FC = 0.75 - 0.24 \cos\varphi .$$

ALB: The albedo of a calm sea surface depends on the solar altitude SALT, and on the fractional diffuse radiation RR = $\frac{\text{Diffuse radiation}}{\text{Direct + diffuse}}$.

As pointed out by Neiburger [19], RR never quite reaches 0 or 1. In this program RR is approximated to $RR = 0.1 + 0.8\ IC$.

The dependence turns out to be linear with RR, the slope depending on the solar altitude SALT [10]. The various slopes from Neumann and Hollman's diagrams [10] were plotted, and a general formula for the slopes found out (see figure 2).

When the albedo for a calm surface is so found, we have to account for roughness and for eventual white caps. The albedo of the foam was estimated at 60%, being somewhat lower than the limit between fresh snow (70 - 95 %) and old snow (45 - 70 %) [11]. This choice is therefore rather arbitrary, and subject to change following any evidence otherwise.

The fraction of the surface covered by foam is, so far, not enough documented. The threshold wind speed for the appearance of white caps is known, [12], [13], [14], but not the fractional area covered by foam at high winds; therefore the following simple form was adopted: (figure 1)

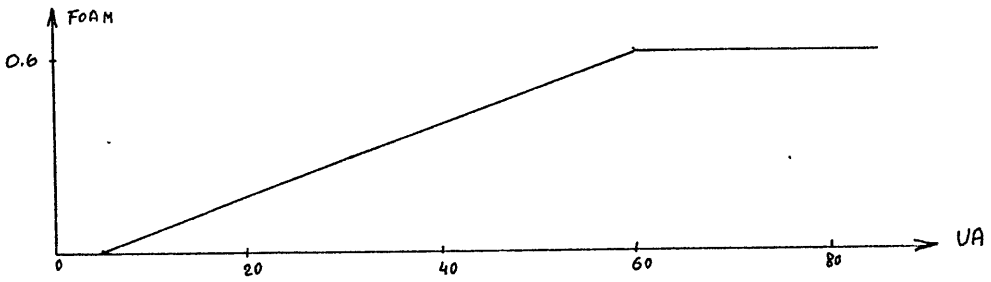

FIG 1: FOAM IS THE FRACTIONAL AREA COVERED BY FOAM.

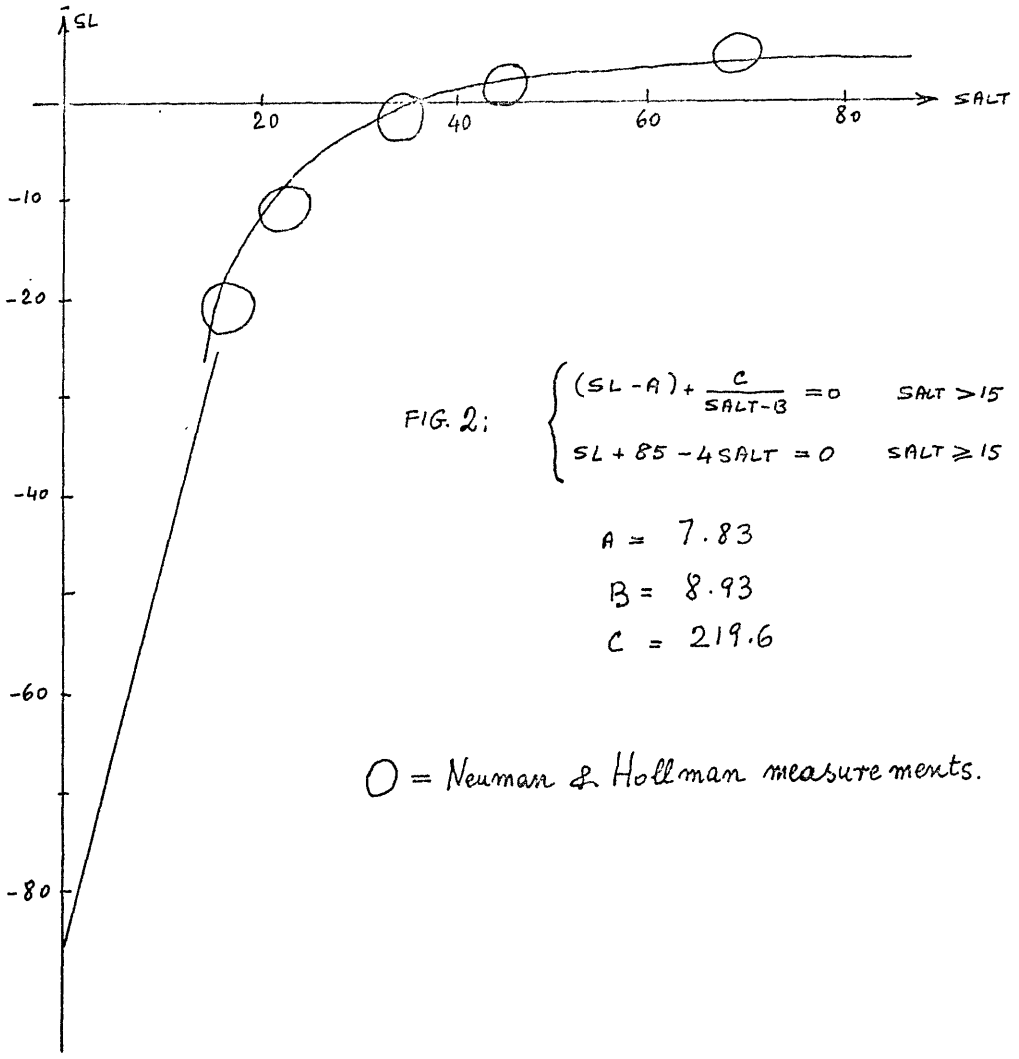

FIG. 2:

$$\begin{cases} (SL - A) + \dfrac{C}{SALT - B} = 0 & SALT > 15 \\ SL + 85 - 4\,SALT = 0 & SALT \geq 15 \end{cases}$$

$A = 7.83$

$B = 8.93$

$C = 219.6$

O = Neuman & Hollman measurements.

The effect of roughness of the sea surface is neglected in this program, since we need accuracy mainly for high SALT, in which case the roughness would not have much effect anyway [18].

RN: $= (S_1 + S_2)(1 - ALB) - RB$,

where S_1 = Direct short wave radiation, S_2 = Diffuse short wave radiation, $(S_1 + S_2)$ is the radiation measured by the pyrheliometer.

The RB is taken as $RB = \sigma T^4$ where σ = St. Boltzman's constant (erroneous in the Smithsonian tables [9]).

The insolation S is continuously measured, however a typical curve looks like:

Using the measured value at the given time (00, 06, 12, or 18, local time) would be misleading for the following reasons:

(i) The variability is so great, due to passing clouds, that each point is not necessarily representative of the average insolation.

(ii) We could smooth out the curve, and thus overcome this difficulty, but even so it wouldn't be accurate enough: the total daily radiation with this method turned out to be appreciably greater than the actual total daily radiation, and this should be the final criterion for the correct form of the S input.

The best method is probably to take a priori the total daily radiation as measured, and assign the whole value to the 12 noon data card, and S = 0 to the other data cards (at 00, 06, and 18). Thus:

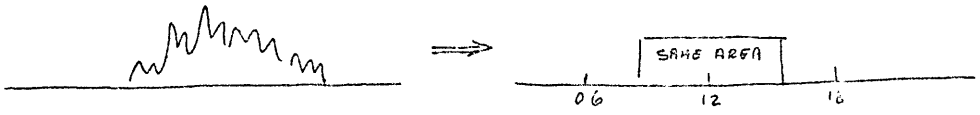

With ALB, RB, and S, the required RN is readily found:

$RN = S(1-ALB) - RB$; In the program RN is given in cal/cm^{2}min, while RNH is given in Kj/m^{2}sec (the proper units in TMS).

QE: The heat loss by evaporation, QE, is given by: QE = L·E; here L = latent heat = (594.9 - .51 x TS) [15], in cal/gm deg; HL is in Kj/ton deg.

QS: The heat loss by sensible heat flux, QS, is given by

$$Qs = \rho_a \cdot C_p \cdot C_{DR} \cdot (T_A - T_S) \cdot UA \; ; \qquad [1], [2]$$

where C_p is here approximated to a constant = 1004 Kj/ton deg, thus neglecting variations with temperature, pressure and relative humidity.

W: At the surface, we have $\tau = \rho_a u_*^2 = \rho_w v_*^2 = \rho_a C_{DR} (UA)^2$;

$\Rightarrow v_*^3 = \left(\frac{\rho_a}{\rho_w} C_{DR}\right)^{3/2} (UA)^3 \equiv C (UA)^3$;

Traditionally, it has been assumed that:

$$W \sim \tau \cdot v_* \qquad [20]$$

so that: $W \approx \rho_w v_*^3 = \rho_w C (UA)^3$.

Turner [16] finds oceanic evidence that W could be as much as 10 times larger, however his work was tentative and undecisive.

Kato and Phillips find out in a more precise laboratory experiment [17] that

$$W = k \tau v_* \quad \text{where} \quad 1 \leq k \leq 1.5 .$$

and they propose $k = 1.25$

In this program, the value 1.25 is adopted.

$$W = 1.25 \, \rho_w C (UA)^3 .$$

REFERENCES:

[1] J. Malkus in The Sea, Hill 1, pp. 106-109.

[2] G. D. Robinson, Q. J. Roy. Met. Soc. 92, pp. 451-464.

[3] Wilson, J. G. R. 65, pp. 3377-3382.

[4] J. Wu, J. G. R. 74, pp. 444-455

[5] Goff and Gratch, Trans. Am. Soc. Heat and Vent. Eng. 52, p. 107.

[6] Haltiner and Martin, Dyn. Met. p. 24.

[7] Berliand and Berliand, Bull. Acad. Sci. USSR (1952)

[8] N. Clark, Ph.D. Thesis, M.I.T., 1967.

[9] Smithsonian Met. Tables, 114, Pub. 4014 (sixth revised edition).

[10] Neumann and Hollman, Union Geod. and Geoph. Int. 10, June, 1961.

[11] Houghton, M.I.T. course 19.72 notes.

[12] Munk, J. M. R. 6, p. 605.

[13] Monaham, J. G. R. 73, p. 1127.

[14] Monaham, J. At. Sci. 26, p. 1026.

[15] Jacobs, Bull. Scripps, 6, p. 30, notation-list.

[16] S. Turner, D. S. R. 16, Fuglister volume, p. 229.

[17] Kato and Phillips, J. F. M. 37, p. 654.

[18] Cox and Munk, J. M. R. 14, p. 71.

[19] Neiburger, Trans. Am. Geoph. Un. 29, pp. 650-652.

[20] Kraus and Turner, Tellus 19, p. 103.

APPENDIX B

OCEANIC MIXING PROGRAM

1. The basic theory

This program computes the changes in the distribution of salinity (S, $^{o}/oo$) and temperature (T, °C) in an oceanic column produced by three processes acting at the surface (z = 0):

H(energy/area time) = upward heat flux across z = 0, including latent heat associated with evaporation

E(length/time) = upward (volume) flux of fresh water across z = 0

W(energy/area time) = rate at which mechanical energy is put into the water column by external (i.e. wind) action.

It is designed to work in fresh and salt water*, and to allow for potential density effects which may be significant in deep columns.

H, E, and W must be supplied as data (the program assumes that H, E, and W do not change in time) in addition to a specification of the initial state of the water column. The latter specification is assumed to be in the form of a series of values of (z_n, T_n, S_n), n = 1, 2, ..., N, where z is the depth (positive downward and $z_1 = 0$.

The pressure p is to some extent a more fundamental variable than z when observation depths are determined by paired protected and unprotected thermometers. Step 1 in the computational procedure

* It won't work when $\left(\frac{\partial \rho}{\partial T}\right)_{PS} = 0$ e.g. fresh water at 4°C.

could be changed to compute z from input values of p, T and S, but the difference would be minor.

The basic assumption is that introduced by Ball (1960), and later used by Krause and Turner (1967) and by Lilly (1968). Ball's argument is for the case W = 0 (and E = 0) and is based on measurements (really orders-of-magnitude) of convective turbulence in the atmospheric surface layer in the daytime over land. When phrased in terms of the ocean, the argument is as follows:

(a) Positive values of H create an unstable stratification near the surface, resulting in a generation of kinetic energy (turbulent) and the formation of a well-mixed layer of depth h(t).

(b) The rate of generation of kinetic energy is given by the vertical integral of $\rho_o \overline{wb}$ where w is the (downward) vertical velocity and b is the negative buoyancy:

$$b \sim g\left(\frac{\rho - \rho_o}{\rho_o}\right) \tag{1}$$

However, the product $\overline{wb}$ is also proportional to the upward heat flux, since $\rho - \rho_o$ is proportional to -T:

$$\rho - \rho_o \sim -\rho_o \alpha T$$

$$\rho_o \overline{wb} = -g\alpha\rho_o \overline{wT} = \frac{\alpha g}{C} H(z)$$

when C is the specific heat. Ball argues that if $\overline{wb}$ had the same sign and magnitude throughout the depth h as it does at z = 0, the

associated rate of generation of kinetic energy in the mixed column,

$$\rho_0 h \overline{wb} \sim \frac{\alpha g}{c} \frac{h}{} H(0)$$

would be so great as to defy any reasonable attempt to balance it by viscous dissipation (or transfer away by gravity waves). He concludes that $\overline{wb}$ must change sign as one leaves $z = 0$, so that

$$\int_0^h \overline{wb}\, dz \sim 0$$

Interpreted literally, now, this means that the potential energy must be unchanged in time as the convection proceeds and h increases:

$$\rho \frac{d}{dt} \left[-\int_0^\infty b z\, dz \right] = 0 \qquad (2)$$

If externally imposed mechanical mixing is present ($W > 0$) it seems reasonable to simply add W to the right side of this equation.

Let $b_e(z)$ represent the distribution of b below the mixed layer h(t) and let $\bar{b}(t)$ represent the uniform b in the mixed layer:

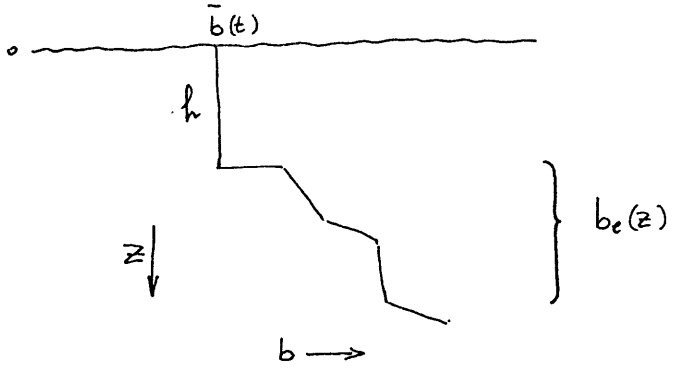

Equation (2) then leads to the relation

$$-\frac{d}{dt}\left(\frac{1}{2}\bar{b}h^2\right) + h\,b_e(h)\frac{dh}{dt} = \frac{W}{\rho_0} \tag{3}$$

The processes H and E change the total temperature and salinity of the column:

$$\frac{d}{dt}(\bar{S}h) - S_e(h)\frac{dh}{dt} = \bar{S}E \quad (\approx S^*E) \tag{4}$$

$$\frac{d}{dt}(\bar{T}h) - T_e(h)\frac{dh}{dt} = -\frac{H}{\rho_0 c} \tag{5}$$

[$\bar{S} = \bar{S}(t)$ on the right-hand side of (4) will, for simplicity, be replaced by a constant S^*.]

We now assume that

$$\rho - \rho_0 = \rho_0(-\alpha T + \beta S) \tag{6}$$

where α and β are constants. Equation (4) and (5) may then be combined to give

$$\frac{d}{dt}(h\bar{b}) - b_e(h)\frac{dh}{dt} = g\left[\beta E S^* + \alpha\frac{H}{\rho_0 c}\right] \equiv G \tag{7}$$

Equations (3) and (7) enable h(t) and $\bar{b}(t)$ to be predicted for given values of W/ρ_0 and G if $b_e(z)$ is known. In our case $b_e(z)$ will be given as a sequence of straight lines connecting the "observed" b's

at the discrete z values, z_n.

Equations (3) and (7) are readily integrated when $b_e(z)$ is a linear function of z. In the following analysis we may imagine that h_n and $h_n + z$ correspond to two consecutive z values, z_n and z_{n+1}, in the original data. Suppose that $t = t_n$ corresponds to the time when h has reached z_n. At this time we have:

In the mixed layer: $\overline{b} = \overline{b}_n$, $\overline{T} = \overline{T}_n$, $\overline{S} = \overline{S}_n$, $h = h_n$

Below h_n: $$b_e(z) = b_n + \frac{z - h_n}{\Delta z} \Delta b \tag{8}$$

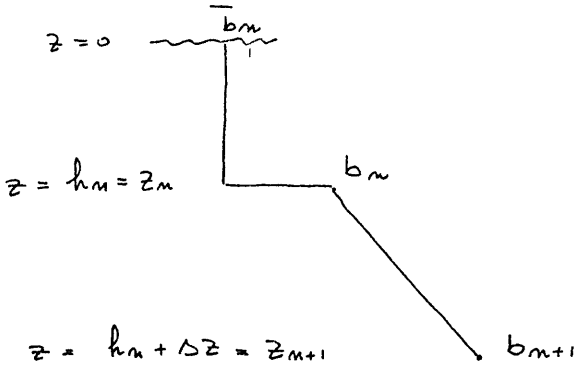

The integrals of (3) and (7) are

$$\overline{b}h^2 - \overline{b}_n h_n^2 - A(h^2 - h_n^2) - \frac{2B}{3}(h^3 - h_n^3) = -2\frac{W}{\rho_o}(t - t_n) \tag{9}$$

$$\overline{b}h - \overline{b}_n h_n - A(h - h_n) - \frac{B}{2}(h^2 - h_n^2) = G(t - t_n) \tag{10}$$

where $A = (b_m \Delta z - h_m \Delta b) \div \Delta z$ and $B = \Delta b \div \Delta z$. These may be combined to give a cubic for h,

$$h^3 + 3\left\{-h_m^2 + \frac{2\Delta z}{\Delta b}\left[h_m(b_m - \bar{b}_m) - G(t-t_m)\right]\right\}$$
$$+ 2\left\{h_m^3 - \frac{3\Delta z}{\Delta b}\left[h_m^2(b_m - \bar{b}_m) + 2\frac{w}{\rho_0}(t-t_m)\right]\right\} = 0 \qquad (11)$$

which could be solved for h(t), and then (9) or (10) could be solved for $\bar{b}(t)$. However, our $b_e(z)$ is given as a succession of linear profiles of the type used in (8), and (11) is only valid until h reaches z_{n+1}. It is then more practical to solve for the time t_{n+1} at which h reaches z_{n+1}. The answer is

$$t_{n+1} = t_n + \frac{(z_{n+1} - z_n)\left[(b_{n+1} - b_n)(2z_n + z_{n+1}) + 6(b_n - \bar{b}_n)z_n\right]}{6\left[z_{n+1}G + 2\frac{w}{\rho_0}\right]} \qquad (12)$$

At this time $\bar{b}$ has changed to

$$\bar{b}_{n+1} = \bar{b}_n +$$
$$+ (z_{n+1} - z_n)\left\{G\cdot\left[(b_{n+1} - b_n)(z_n + 2z_{n+1}) + 3(b_n - \bar{b}_n)(z_n + z_{n+1})\right] + \right. \qquad (13)$$
$$\left. + \frac{w}{\rho_0}\left[6(b_n - \bar{b}_n) + 3(b_{n+1} - b_n)\right]\right\} \Big/ 3z_{n+1}\left[z_{n+1}G + 2\frac{w}{\rho_0}\right].$$

The corresponding changes in salinity and temperature in the mixed layer are readily computed from (4) and (5) [assuming that S_e and T_e vary linearly with z].

$$\overline{S}_{m+1} = \left[z_m \overline{S}_m + \tfrac{1}{2}(z_{m+1} - z_m)(S_m + S_{m+1}) + (t_{m+1} - t_m)\, E\, S^* \right] \Big/ z_{m+1} \qquad (14)$$

$$\overline{T}_{m+1} = \left[z_m \overline{T}_m + \tfrac{1}{2}(z_{m+1} - z_m)(T_m + T_{m+1}) - (t_{m+1} - t_m) \frac{H}{\rho_0 c} \right] \Big/ z_{m+1} \qquad (15)$$

In this way the program will compute the length of time it will take the given values of H, E, and W to extent the mixed layer down past each of the successive initial data points z_n; and the values of $\overline{T}$ and $\overline{S}$ which occur in the mixed layer at those times. At the start it will be assumed that $h_1 = z_1 = 0$, $\bar{b}_1 = b_1$, $\overline{S}_1 = S_1$ and $\overline{T}_1 = T_1$ (the surface values of z, b, S and T).

It may happen in the original data that b will occasionally decrease downward [typically, when T and S are so uniform that small observational errors can corrupt the (presumably) monotonic increase of b downward]. Although this could be "corrected" by smoothing of the original data, such a procedure is arbitrary. Furthermore, under these circumstances, the mixed layer will pass quickly by such a region perhaps even giving $t_{n+1} < t_n$! In general, this type of irregularity will not interfere with the overall conclusions to be drawn from the computation, and no special treatment will be given it.

It may also happen that one wishes to allow E, H and W to change with time. This can be done by successive computations in

which the input data for a second run (with changed H, E, W) is artificially reconstituted from the results of a first run.

2. Modification for compressibility

One minor complication must yet be described; in some critical cases of possible interest when T_e and S_e are almost constant, the compressibility of water must be allowed for in computing the buoyancy. This can be done most simply by

(a) Computing a reference isentropic state $(\tilde{\tilde{\ }})$

$$S = \text{constant} = \text{mean salinity} = \tilde{\tilde{S}}$$
$$T = \tilde{\tilde{T}}(z) \qquad (16)$$
$$\rho = \tilde{\tilde{\rho}}(z)$$

(b) Computing the initial b distribution from

$$b = g\,\frac{\rho - \tilde{\tilde{\rho}}}{\tilde{\tilde{\rho}}} \qquad (17)$$

where ρ is computed rigorously, i.e. not from (6).

(c) (6), with its α and β, is then used only to enable changes in $\int b\,dz$ to be computed from H and E via (4) and (5).

This modification for compressibility is equivalent to that which is necessary in using the "Boussinesq" system to study atmospheric

motions which are more than about 10 meters (but not more than 3 km) in vertical scale height. Under those circumstances the buoyancy (now counted positive upward) is given by

$$b = g\left(\frac{T - T_a(z)}{T_o}\right) \sim -g\left(\frac{\rho - \rho_a}{\rho_a}\right) \tag{18}$$

where $T_a = T_o - \frac{g}{c_p} z$ is the adiabatic stratification for a perfect gas. It is only when the scale height of the motion is so small that T_a is a constant that b for a gas can be simplified to $g(T/T_o - 1)$. The usual oceanographic situation corresponds to the latter circumstance; what (16) and (17) do is to allow for ocean compressibility in a manner similar to that in which (18) acts in the atmosphere.

References

Fofonoff, N. P., 1962: Physical properties of sea water. Pages 3-29 in The Sea, vol. I., M. Hill (ed.) Interscience, New York.

Eckart, C., 1958: Properties of water, part II. Amer. J. Sci., 256 (April), 225-240.

Ball, F. K., 1960: Control of inversion height by surface heating. Quart. J. Roy. Meteor. Soc., 86, 483-94.

Kraus, E., and J. Turner, 1967: A one-dimensional model of the seasonal thermocline. Part II. The general theory and its consequences. Tellus, 19, 98-106.

Lilly, D. K., 1968: Models of cloud-topped mixed layers under a strong inversion. Quart. J. Roy. Meteor. Soc., 94 292-309.